Isotope geochemistry and revised geochronology of the Purrido Ophiolite (Cabo Ortegal Complex, NW Iberian Massif): Devonian magmatism with mixed sources and involved Mesoproterozoic basement

SONIA SÁNCHEZ MARTÍNEZ[1], RICARDO ARENAS[2]*, AXEL GERDES[1], PEDRO CASTIÑEIRAS[2], ALAIN PETREL[3] & JAVIER FERNÁNDEZ-SUÁREZ[2]

[1]*Institut für Geowissenschaften, Goethe Universität, D-6438 Frankfurt am Main, Germany*

[2]*Departamento de Petrología y Geoquímica e Instituto de Geología Económica (CSIC), Universidad Complutense, 28040 Madrid, Spain*

[3]*CREAIT NETWORK, Department of Earth Sciences, Memorial University of Newfoundland, St. John's, NL, A1B 3X5, Canada*

**Corresponding author (e-mail: arenas@geo.ucm.es)*

Abstract: In the Purrido Ophiolite (Cabo Ortegal Complex), new U–Pb zircon dating of the amphibolite G03-8 (by laser ablation inductively coupled plasma mass spectrometry) confirms the existence of a dominant Mesoproterozoic zircon population with a refined age of 1155 ± 14 Ma. However, the U–Pb zircon dating of two more amphibolite samples (by sensitive high-resolution ion microprobe) has provided new ages of 395 ± 3 Ma and 395 ± 2 Ma, respectively, interpreted as the crystallization age. Hf isotope data for zircon show that most of the Devonian zircons crystallized from a juvenile depleted mantle source. The Mesoproterozoic zircons have relatively juvenile Hf isotopic composition reflecting some influence of an older component. A few Devonian zircon crystals show evidence of mixing with an older component represented by the Mesoproterozoic zircons. The whole-rock Sm–Nd isotope data indicate an important heterogeneity in the composition of the Purrido amphibolites, only compatible with the generation of their protoliths from two sources. We interpret these puzzling data as resulting from the mixing of a Devonian mantle-derived magma with a Mesoproterozoic basement. These new data provide new perspectives in the interpretation of the most common ophiolites across the Variscan suture in Europe.

The Variscan Belt is an orogen formed during the final event related to the assembly of Pangaea, in Devonian and Carboniferous times (Fig. 1; Matte 1991; Martínez Catalán *et al.* 2009). The main suture in this belt is preserved in several exotic complexes with ophiolites and terranes affected by high-pressure metamorphism (Martínez Catalán *et al.* 2007; Fig. 1), interpreted as erosive remnants of a gigantic stacking of nappes (Ries & Shackleton 1971; Arenas *et al.* 1986). In the NW of the Iberian Massif, the Variscan suture is rootless and can be followed through the Cabo Ortegal and Órdenes complexes to the Malpica Tui unit. The suture is highlighted by the presence of several ophiolitic units with a wide regional distribution (Fig. 2; Arenas *et al.* 2007*a*). These ophiolites are considered to represent remnants of the Rheic Ocean, the oceanic domain that closed during the convergence between Gondwana and Laurussia (Stampfli & Borel 2002; Winchester *et al.* 2002; Murphy *et al.* 2006; Nance *et al.*, 2010). They show important lithological and geochronological variations and record relevant information about the evolution of the Rheic Ocean, from the initial rifting and opening of the ocean until the final stages of its closure. Some mafic formations incorporated into the suture zone have been interpreted as remnants of peri-Gondwanan oceanic domains predating the opening of the Rheic Ocean; that is, remnants of the Iapetus or Tornquist ocean (Sánchez Martínez *et al.* 2009).

Two main groups of ophiolites have been identified in NW Iberia, the lower and the upper ophiolitic units (Fig. 2). There is a third unit with ophiolitic affinities formed by a thick serpentinitic mélange, the Somozas mélange (Arenas *et al.* 2009), which appears in a frontal position in the allochthonous pile defined by the exotic terranes (Fig. 2). The lower ophiolitic units contain thick sections of typical greenschists with some interbedded phyllites and pelitic schists and some small lenses of sheared metagabbros; they also include some thin layers of ultramafic rocks and tonalitic orthogneisses. The mafic rocks are characterized by compositions equivalent to island-arc tholeiites (Vila de Cruces unit), and they can be considered as mafic successions generated in a suprasubduction context. Dating of a metre thick layer of orthogneisses interbedded between mafic schists in the Vila de Cruces unit at 497 ± 4 Ma (U Pb on zircon by isotope dilution thermal ionization mass spectrometry (ID-TIMS)) allows the interpretation of these ophiolites as lithological successions generated during the initial stages of the opening of the Rheic Ocean (Arenas *et al.* 2007*b*). The lower ophiolitic units can be thus considered as mafic back-arc sequences generated in a context of continuous extension, which took place during the rifting from Gondwana of Avalonia and other related peri-Gondwanan terranes with arc affinity. These terranes drifted to the north during the progressive widening of the Rheic Ocean.

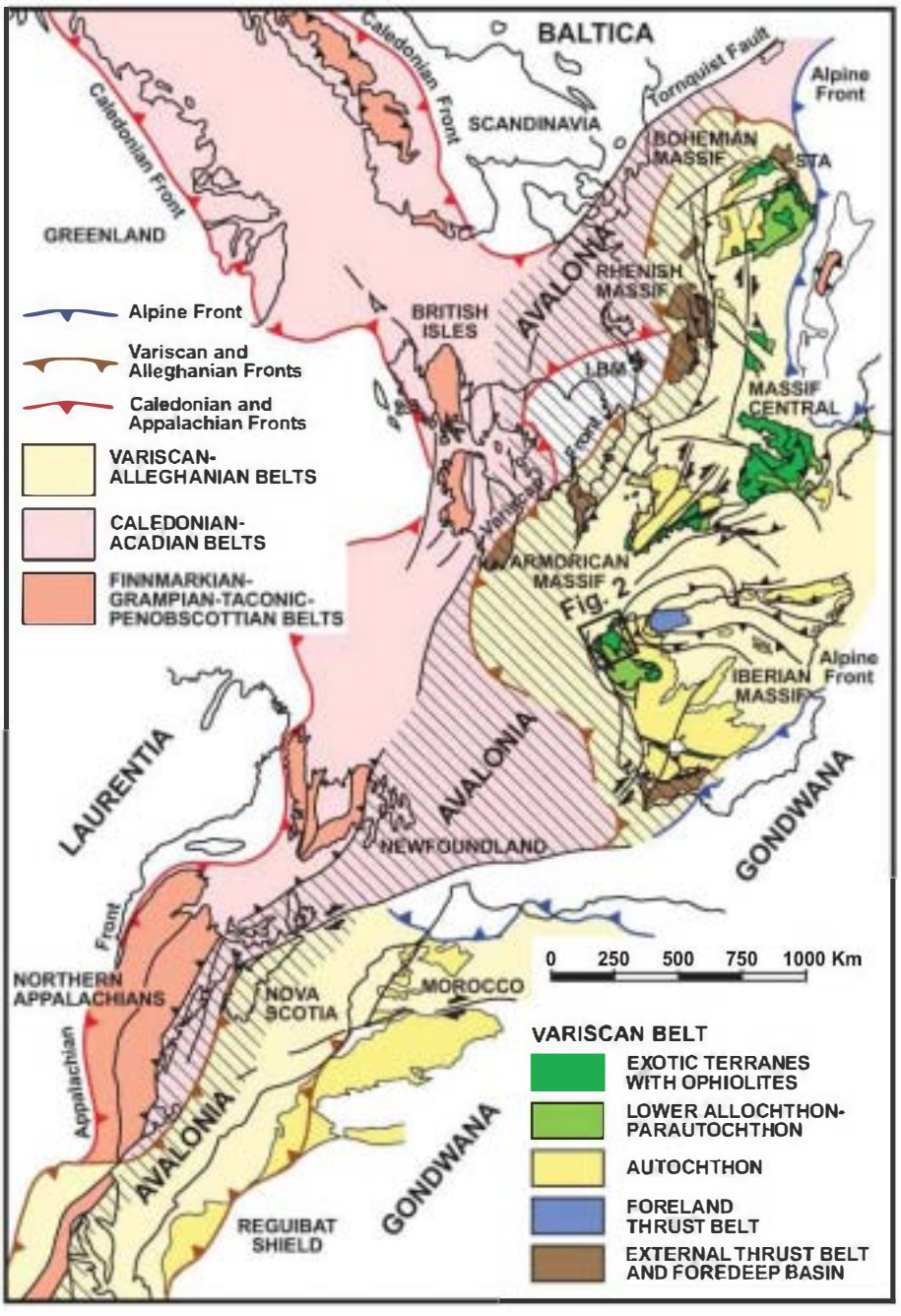

Fig. 1. Sketch showing the distribution of the Palaeozoic orogens in a reconstruction of the Baltica Laurentia Gondwana junction that developed during the assembly of Pangaea. The distribution of the most important domains described in the Variscan Belt is also shown, together with the inferred position of the microcontinent Avalonia and the study region in NW Iberia. LBM, London Brabant Massif; STA, Silesian Terrane Assemblage.

The upper ophiolites consist of ultramafic rocks, gabbros, amphibolites and diabase dykes, and are devoid of volcanic or sedimentary rocks. These ophiolites show characteristics similar to those exhibited by oceanic lithosphere generated in extensional settings located above subduction zones. An important extension event is indicated by the presence of a swarm of diabase dykes intruding the ophiolite at different structural levels, including the mantle ultramafic section (Díaz García *et al.* 1999). The geochemical features of these ophiolites are also typical of a suprasubduction-zone setting, as they resemble island-arc tholeiites with negative Nb anomalies (Pin *et al.* 2002; Sánchez Martínez *et al.* 2009). Some metagabbros of the Careón ophiolite, the most characteristic upper ophiolite located in the SE of the Órdenes Complex (Fig. 2), have been dated at 395 ± 2 Ma (U–Pb on zircon by ID-TIMS; Díaz García *et al.* 1999; Pin *et al.* 2002). Other similar and related ophiolites

Fig. 2. Terrane distribution in the allochthonous complexes of NW Iberia (Galicia) and a WNW–ESE-oriented general cross-section. The map shows the synformal structure of the complexes where a rootless branch of the main Pangaea suture in Europe is exposed. The Purrido unit is a member of the upper ophiolitic units located in the western part of the Cabo Ortegal Complex. The location of the geological map presented in Figure 3 is also shown.

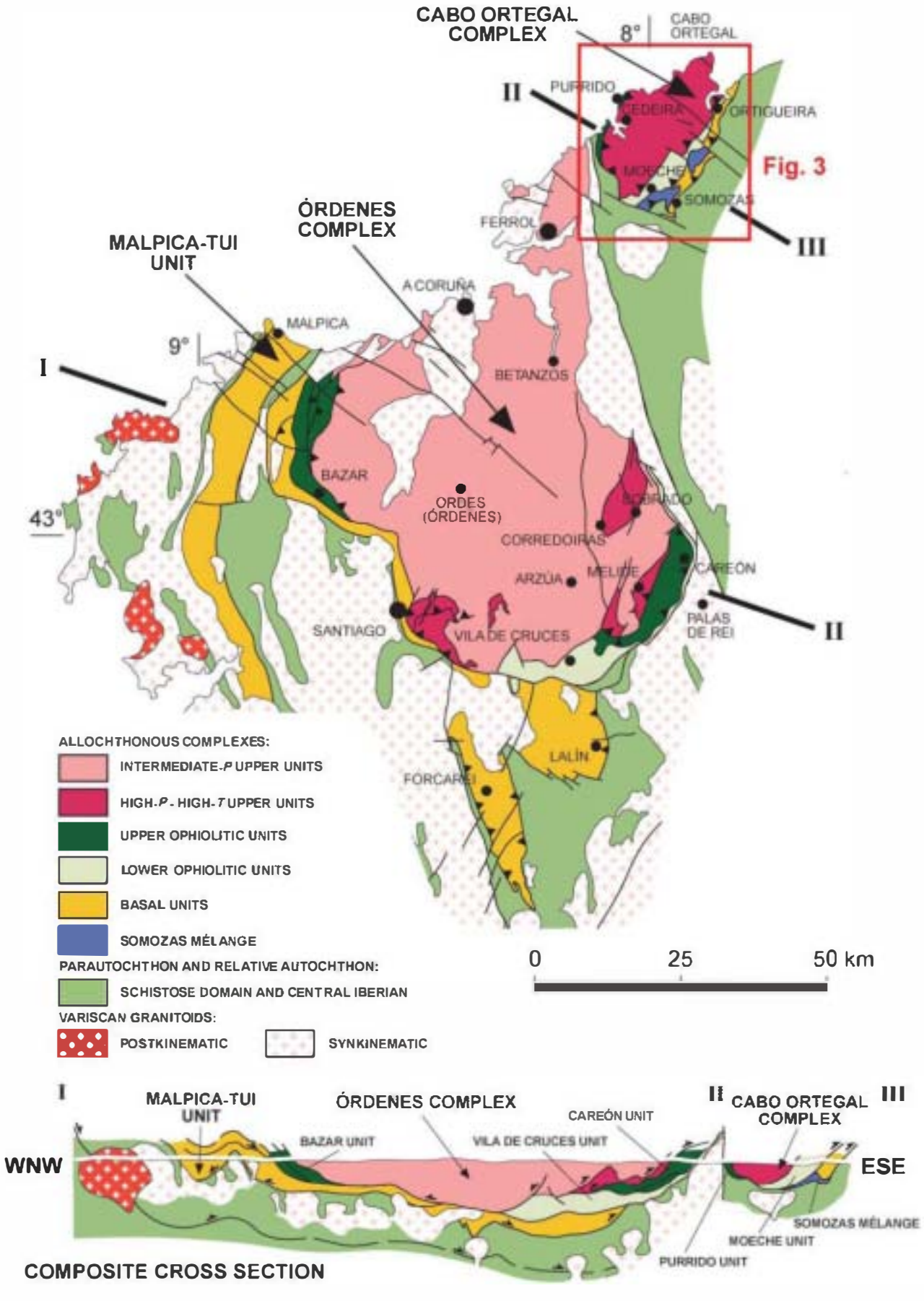
CABO ORTEGAL COMPLEX
8°
CABO ORTEGAL
II
PURRIDO
CEDEIRA
ORTIGUEIRA
Fig. 3
MOECHE
SOMOZAS
FERROL
III
ÓRDENES COMPLEX
MALPICA-TUI UNIT
A CORUÑA
MALPICA
9°
I
BETANZOS
BAZAR
ORDES (ÓRDENES)
43°
CORREDOIRAS
ARZÚA
MELIDE
CARBALLO
CAREÓN
SANTIAGO
VILA DE CRUCES
PALAS DE REI
II
LALÍN
FORCAREI
ALLOCHTHONOUS COMPLEXES:
INTERMEDIATE-P UPPER UNITS
HIGH-P - HIGH-T UPPER UNITS
UPPER OPHIOLITIC UNITS
LOWER OPHIOLITIC UNITS
BASAL UNITS
SOMOZAS MÉLANGE
PARAUTOCHTHON AND RELATIVE AUTOCHTHON:
SCHISTOSE DOMAIN AND CENTRAL IBERIAN
VARISCAN GRANITOIDS:
POSTKINEMATIC
SYNKINEMATIC
0
25
50 km
I
MALPICA-TUI UNIT
ÓRDENES COMPLEX
II
CABO ORTEGAL COMPLEX
III
CAREÓN UNIT
BAZAR UNIT
VILA DE CRUCES UNIT
WNW
ESE
SOMOZAS MÉLANGE
MOECHE UNIT
PURRIDO UNIT
COMPOSITE CROSS SECTION

located in the Portuguese region of Trás-os-Montes, included in the Morais Complex, yielded similar U–Pb zircon ages (Pin *et al.* 2006). The generation of suprasubduction-zone oceanic lithosphere in Devonian times has been interpreted as related to the activity of an intra-oceanic subduction zone dipping to the north, in the context of a contracting Rheic Ocean (Sánchez Martínez *et al.* 2007*a*; Gómez Barreiro *et al.* 2010). This Devonian oceanic lithosphere is the youngest lithosphere generated in the realm of the Rheic Ocean, and its juvenile and buoyant character would explain a rapid accretion to the margin of Laurussia and its preservation as the most common ophiolitic type in the suture of the European Variscan Belt (Sánchez Martínez *et al.* 2007*a*).

Some metagabbros with dominant populations of Mesoproterozoic zircons have been recently reported in ophiolites of the Cabo Ortegal and Órdenes complexes. These zircons were interpreted as orthomagmatic in the mafic rocks and they were used to obtain the chronology of the igneous protolith (Sánchez Martínez *et al.* 2006, 2009; Sánchez Martínez 2009). The protolith of one sample of metagabbroic amphibolite from the Purrido unit was dated at 1159 ± 39 Ma, and the protoliths of two greenschist-facies metagabbros from the Vila de Cruces unit were dated at 1176 ± 85 and 1168 +14/−50 Ma, respectively (U–Pb on zircon; laser ablation inductively coupled plasma mass spectrometry (LA-ICP-MS)). These surprising data were used to interpret the Purrido unit as a pre-Rodinian ophiolite, preserved for a long time owing to its inclusion in a back-arc basin attached to the Gondwanan margin (Sánchez Martínez *et al.* 2006). The Vila de Cruces unit could have a more complex interpretation, because, as mentioned above, it also includes Palaeozoic lithologies. This unit was later interpreted as a composite terrane in which a Mesoproterozoic basement was involved (Sánchez Martínez *et al.* 2009). Murphy & Gutiérrez-Alonso (2008) suggested that the Purrido Ophiolite is also a composite body that, in addition to the Mesoproterozoic rocks, is characterized by a juvenile Sm–Nd isotopic signature at *c.* 395 Ma (the more common age for the upper ophiolites). Murphy *et al.* (2008) have suggested the general presence of a Mesoproterozoic basement in the peri-Gondwanan realm represented in NW Iberia. This basement would be resting over a fossil Mesoproterozoic lithospheric mantle.

However, despite the gechronological data outlined above, fundamental questions remain concerning the age and significance of these units. The reason for this uncertainty is the small number of dated samples, the scarcity of zircon in most samples and the ambiguous interpretation of zircon features (orthomagmatic v. inherited). This study addresses the ambiguity in the age of the Purrido Ophiolite by presenting additional U–Pb zircon data from selected amphibolite lithologies. The new U–Pb data are combined with whole-rock Sm–Nd and zircon Lu–Hf isotope data to differentiate between inherited and orthomagmatic zircon grains, subsequently allowing us to reinterpret the age of the Purrido Ophiolite. The new data do not support the previous interpretation of the Purrido unit as a Mesoproterozoic ophiolite. However, our data clearly show a complex history for the generation of the mafic rocks of the Purrido unit, which involves the participation of at least two sources with very different ages. These data open new perspectives for the interpretation of some of the ophiolites involved in the Variscan Belt.

The Purrido Ophiolite of the Cabo Ortegal Complex

The Purrido unit is located in the westernmost part of the Cabo Ortegal Complex (Fig. 3). It consists of a 300 m thick series of common amphibolites and garnet amphibolites that show a relatively homogeneous mafic composition. However, some differences in the proportion of plagioclase or amphibole, the grain size, the development of tectonic banding and the intensity of shearing can be observed in different exposures. The Carreiro shear zone is located above the Purrido unit. This shear zone represents the thrust contact of the upper units of the allochthonous complexes, interpreted as an arc-derived terrane with peri-Gondwanan provenance (see Abati *et al.* 2007; Díaz García *et al.* 2010; Fuenlabrada *et al.* 2010; and references therein). The Purrido amphibolites were first described by Vogel (1967) and mapped again recently by Azcárraga (2000). Sánchez Martínez *et al.* (2007*b*) presented the first geochemical study, based on 18 amphibolites from this unit, the protoliths of which were initially correlated with those of the Careón ophiolite and thus considered of Devonian age. The most common amphibolites have typical basaltic compositions with minor variation in the chemistry of the major elements and REE. A larger variation can be observed in the trace element composition, although all the studied samples can be classified as typical island-arc tholeiites with slightly negative Nb anomalies. Figure 4 shows some of the most significant geochemical features of these amphibolites and a general column showing the most relevant lithologies and their internal distribution. In relation to the chronology of the Purrido unit, Sánchez Martínez *et al.* (2006) presented the U–Pb dating of zircon from a sample of common amphibolites (sample G03-8; LA-ICP-MS). Twenty-three U–Pb analyses were performed on 21 zircon grains, obtaining a coherent group of 10 analyses with a mean age of 1159 ± 39 Ma, interpreted as the crystallization age for the protoliths of this metagabbro. This sample also contained a zircon group with older Mesoproterozoic ages ranging between 1265 ± 8 Ma and 1658 ± 32 Ma, interpreted as inherited zircons.

U–Pb zircon geochronology

The samples used in this study were taken during two field campaigns (2003 and 2007). In most cases 15–20 kg of amphibolite were sampled, and subsequently processed by conventional methods for zircon separation. Zircon output was generally poor, as is typical in mafic rocks, with fewer than tens of grains extracted from the full sample collected. The sampling localities were as follows (Fig. 3): Purrido Mount quarry (43°42'20"N, 8°03'10"W), samples G07-1 and G07-2; contact of the Carreiro shear zone (43°42'40"N, 8°02'45"W), sample G07-4; Baleo beach (43°38'50"N, 8°06'10"W), samples G07-5 and G07-6; Chirlateira Point (43°39'30"N, 8°05'25"W), samples G03-7 and G07-7. Within this group, samples G07-4, G07-5 and G07-6 did not contain any zircon, or they yielded very few grains, insufficient for secondary ionization mass spectrometry (SIMS) U–Pb geochronology. The other samples provided enough zircon grains and were analysed by sensitive high-resolution ion microprobe (SHRIMP) in July 2008 (SUMAC facility, USGS–Stanford University), following U–Th–Pb analytical procedures

Fig. 3. Geological map and cross-section of the Cabo Ortegal Complex. The location of the samples used in this study for isotope geochemistry and U–Pb dating (G samples), and the localities sampled in the Purrido Ophiolite are also shown.

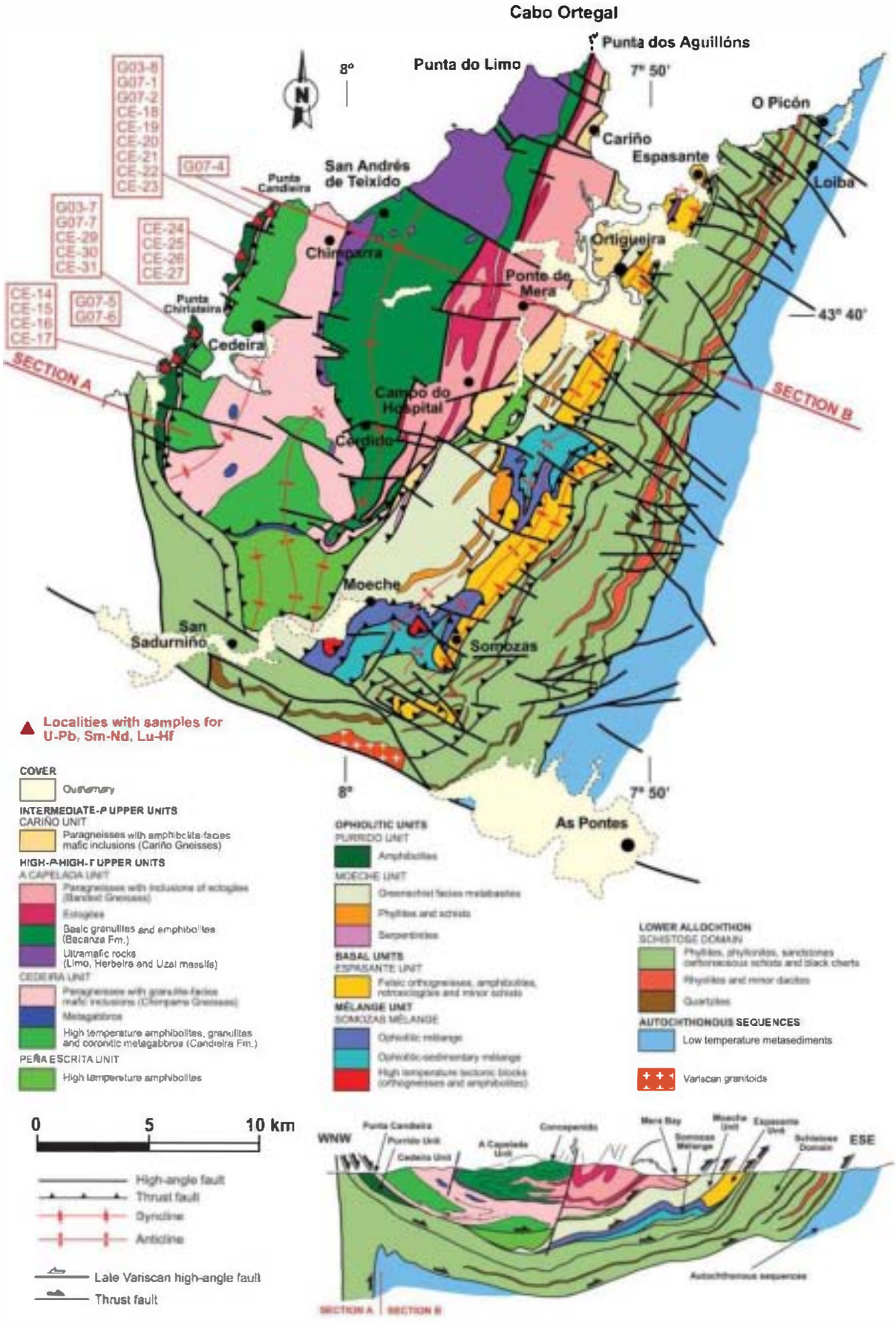
Cabo Ortegal
Punta dos Aguillóns
Punta do Limo
8°
7° 50'
O Picón
Cariño
Espasante
Loiba
San Andrés de Teixido
Punta Candieira
Ortigueira
Ponte de Mera
Punta Chirlateira
Cedeira
43° 40'
SECTION A
SECTION B
Campo do Hospital
Cerdido
Moeche
San Sadurniño
Somozas
As Pontes
G03-8
G07-1
G07-2
CE-18
CE-19
CE-20
CE-21
CE-22
CE-23
G07-4
G03-7
G07-7
CE-29
CE-30
CE-31
CE-24
CE-25
CE-26
CE-27
CE-14
CE-15
CE-16
CE-17
G07-5
G07-6
Localities with samples for U-Pb, Sm-Nd, Lu-Hf
COVER
Quaternary
INTERMEDIATE-P UPPER UNITS
CARIÑO UNIT
Paragneisses with amphibolite-facies mafic inclusions (Cariño Gneisses)
HIGH-P/HIGH-T UPPER UNITS
A CAPELADA UNIT
Paragneisses with inclusions of eclogites (Banded Gneisses)
Eclogites
Basic granulites and amphibolites (Bacanza Fm.)
Ultramafic rocks (Limo, Herbeira and Uzal massifs)
CEDEIRA UNIT
Paragneisses with granulite-facies mafic inclusions (Chimparra Gneisses)
Metagabbros
High temperature amphibolites, granulites and coronitic metagabbros (Candieira Fm.)
PEÑA ESCRITA UNIT
High temperature amphibolites
OPHIOLITIC UNITS
PURRIDO UNIT
Amphibolites
MOECHE UNIT
Greenschist facies metabasites
Phyllites and schists
Serpentinites
BASAL UNITS
ESPASANTE UNIT
Felsic orthogneisses, amphibolites, retroeclogites and minor schists
MÉLANGE UNIT
SOMOZAS MÉLANGE
Ophiolitic mélange
Ophiolitic-sedimentary mélange
High temperature tectonic blocks (orthogneisses and amphibolites)
LOWER ALLOCHTHON
SCHISTOSE DOMAIN
Phyllites, phyllonites, sandstones carbonaceous schists and black cherts
Rhyolites and minor dacites
Quartzites
AUTOCHTHONOUS SEQUENCES
Low temperature metasediments
Variscan granitoids
0
5
10 km
High-angle fault
Thrust fault
Syncline
Anticline
Late Variscan high-angle fault
Thrust fault
WNW
ESE
Punta Candieira
Purrido Unit
Cedeira Unit
A Capelada Unit
Concepenido
Mera Bay
Moeche Unit
Somozas Mélange
Espasante Unit
Schistose Domain
Autochthonous sequences
SECTION A
SECTION B

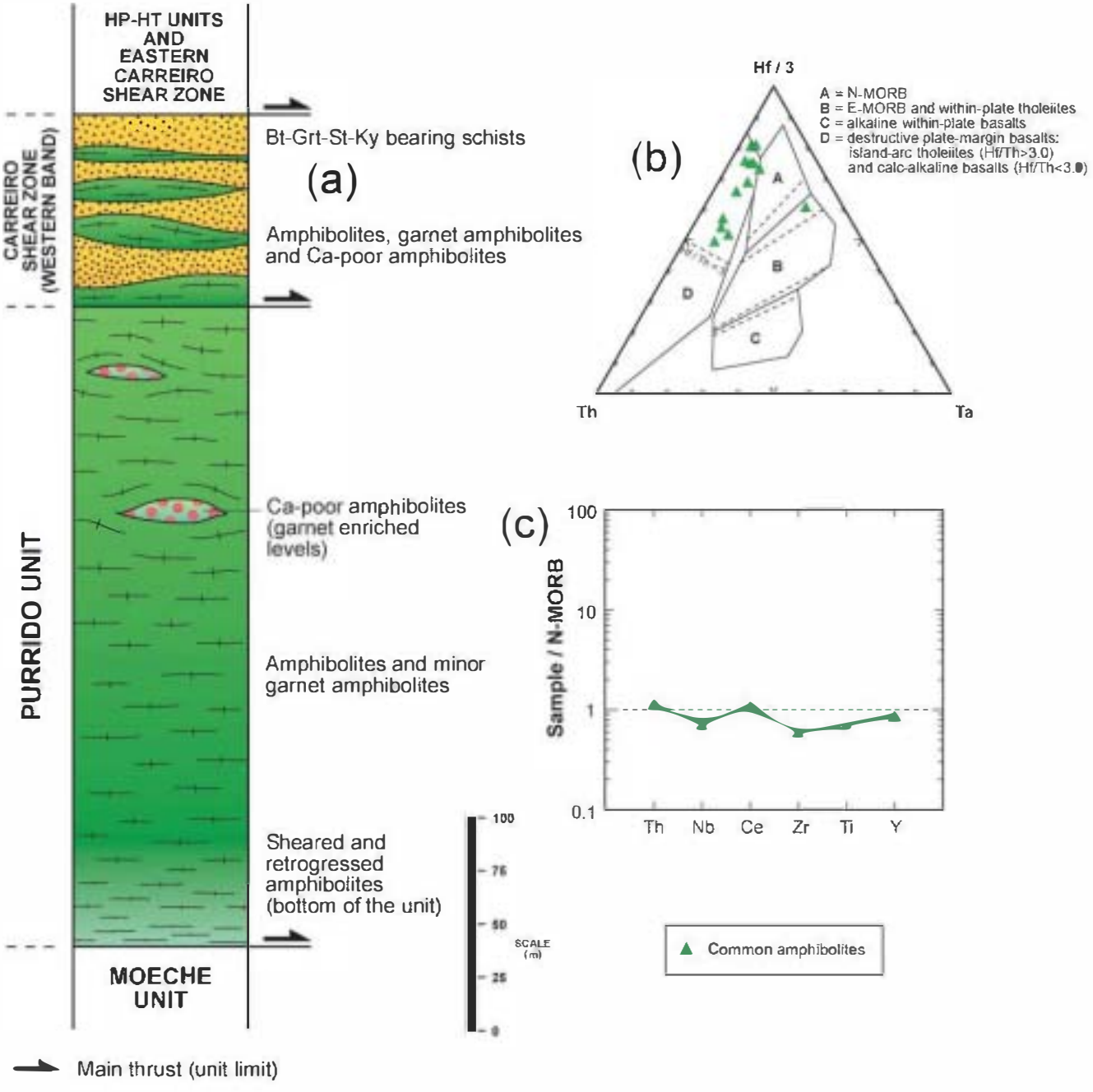

Fig. 4. Lithological constitution and geochemistry of the Purrido Ophiolite. (a) Characteristic section of the unit. (b) Th Hf Ta diagram (Wood 1980) with the projection of the most representative common amphibolites. E-MORB, enriched MORB. (c) Normal mid-ocean-ridge basalt (N-MORB)-normalized trace element pattern of the common amphibolites (average composition); selected elements and normalizing values according to the criteria of Pearce (1996).

for zircon dating described by Williams (1997). None of the zircons analysed by SHRIMP reproduced the Mesoproterozoic ages obtained previously in sample G03-8 (Sánchez Martínez *et al.* 2006). As a result, we decided to analyse once again the zircons from sample G03-8 using the same method as in the original research: U–Pb on zircon by LA-ICP-MS. These new analyses were obtained in March 2009 (Goethe University Frankfurt), following U–Th–Pb analytical procedures for zircon dating described by Frei & Gerdes (2009) and Gerdes & Zeh (2006, 2009).

SHRIMP geochronology: sample description and results

G07-1. Most of the zircon grains from this sample are subidiomorphic prisms with rounded edges and breadth-to-length ratios around 1:2 or 1:3. Some of the prisms are broken and there are also a few small rounded crystals. Under cathodoluminescence (CL), they exhibit an assortment of textures (Fig. 5), typical of both magmatic and metamorphic zircon (Corfu *et al.* 2003), which can be divided in four groups. The first group comprises the grains that show a combination of oscillatory and sector

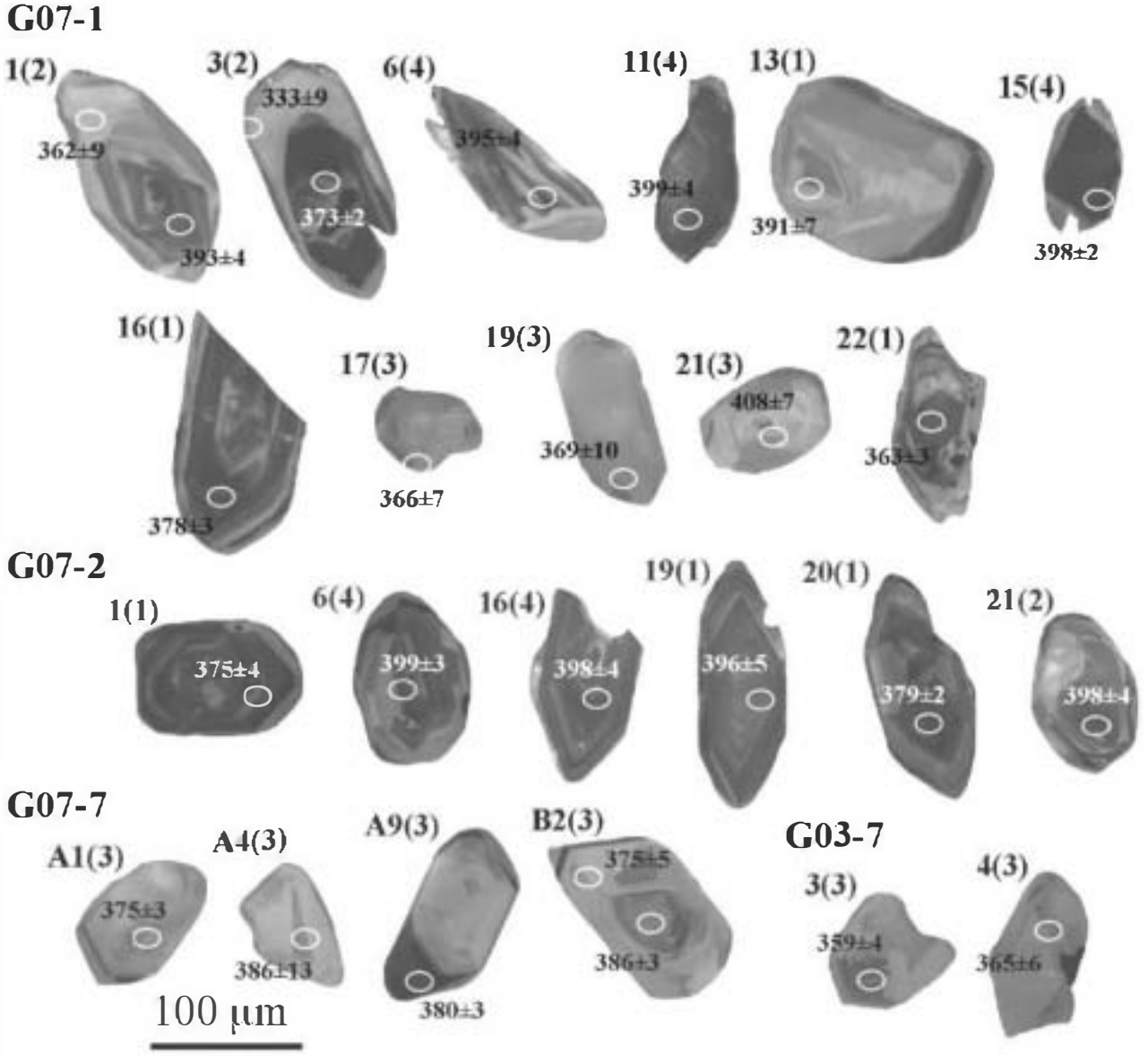

Fig. 5. Cathodoluminescence images for selected zircons from samples G07-1, G07-2, G07-7 and G03-7. The numbers in parenthesis denote the textural group.

zoning that is truncated by dissolution and with no clear evidence of metamorphic overgrowth or inherited xenocrystic cores (grains 13, 16 and 22, Fig. 5). The second group includes zircon with characteristics of the first group that exhibit an overgrowth after dissolution. These rims exhibit a homogeneous or sector zoning and they are more luminescent than the oscillatory and sector zoned cores (grains 1 and 3, Fig. 5). The third group is composed of a few luminescent small grains with sector or homogeneous zoning (grains 17, 19 and 21, Fig. 5). The fourth group is made up of other zircon crystals that are less luminescent and have thin and discontinuous luminescent rims (grains 6, 11 and 15, Fig. 5).

Twenty-six analyses were performed on 23 zircon grains, yielding ages that extend from 415 to 333 Ma. Zircon from group 1 and cores from group 2 yield ages from 415 to 363 Ma. Zircon from group 3 and rims from group 2 have systematically young ages (from 369 to 333 Ma), except for two grains from group 3 that yield old ages (analyses 10 and 21; 395 and 408 Ma, respectively). Four core analyses on zircon grains from group 4 yield similar ages (analyses 2, 6, 11 and 15; *c.* 395 Ma), whereas another core analysis from this group yields a younger age (analysis 4; *c.* 375 Ma). Almost all the Th/U ratios are higher than 0.1; only two young analyses from group 3 (analyses 17 and 19) have lower Th/U ratios (0.08).

G07-2. Zircon grains extracted from this sample are virtually identical to those of sample G07-1; they are prisms and small rounded grains that can be divided into four groups according to their CL textures. In this sample, group 1 zircons are the most abundant, whereas group 2 zircons are scarce. Twenty-seven

zircon grains were analysed and the geochronological results are equivalent to those of sample G07-1, with a variation between 409 and 359 Ma. Group 1 zircon and a core from group 2 vary in age between 398 and 359 Ma. Group 3 zircons yield indistinguishable ages around 380 Ma, whereas core analyses from group 4 zircons range from 409 to 372 Ma. In this sample, all the Th/U ratios are higher than 0.1.

G07-7. Most of the zircon grains from this sample have lower breadth-to-length ratios than the previous samples and the CL images reveal that they correspond to group 3, luminescent grains with sector or homogeneous textures. In some cases, the luminescent grains have non-luminescent tips with homogeneous zoning (grains 3 and 9, Fig. 5). Nineteen analyses were performed on 15 zircon grains and most of the analyses cluster around a mean age 378 ± 3 Ma. A more accurate age can be calculated using 14 analyses, which yield a lower intercept of 379 ± 2 Ma (MSWD = 1.3), anchored at $^{207}Pb/^{206}Pb = 0.861 \pm 0.001$ (Fig. 6a). Compositionally, zircon from this sample is different, as it exhibits low U and Th contents, inducing higher uncertainties in the isotopic ratios (Fig. 6a). Low Th/U ratios together with the CL characteristics of the zircon crystals suggest a metamorphic origin for them (Fig. 7).

G03-7. Only four zircon grains were recovered from this sample, and they are similar to those of sample G07-7 in habit, CL characteristics (group 3) and composition (low Th/U ratios, Fig. 7). One analysis (number 1.1) has a large error probably owing to its low U and high common Pb content (0.3 ppm and 4.64%, respectively). The other five analyses performed on this sample yield a lower intercept of 365 ± 5 Ma (MSWD = 1.3), anchored at $^{207}Pb/^{206}Pb = 0.861 \pm 0.001$ (Fig. 6b).

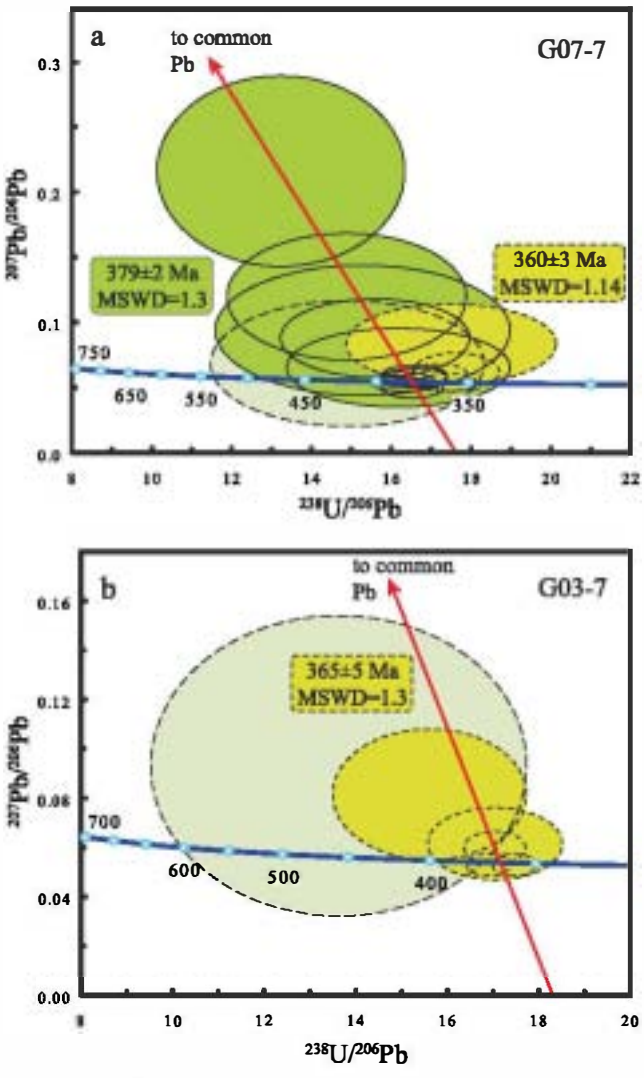

Fig. 6. Tera–Wasserburg plot showing SHRIMP zircon analyses from samples (**a**) G07-7 and (**b**) G03-7. Continuous-line ellipses represent metamorphic ages. Dotted-line ellipses represent lead loss ages. Dashed-line ellipses are not considered in calculating the age. Error ellipses are $\pm 2\sigma$.

Interpretation of the SHRIMP results

In spite of the similar zoning patterns found in the zircons from samples G07-1 and G07-2, the results obtained for these samples clearly show that in most cases there is no simple match between CL features, Th/U ratio and age. Accordingly, we cannot base our interpretation of the geochronological data entirely on these textural and compositional characteristics and we must rely on additional information, such as the results of the other two samples and the previous geochronology. In a preliminary evaluation of the data from samples G07-1 and G07-2, it is evident that the age distribution is prolonged (between 50 and 70 Ma) and it probably corresponds to more than one geological event. Using a statistical approach, the Sambridge Compston algorithm included in Isoplot (Ludwig 2003), it is possible to discriminate two major age components at *c.* 395 and *c.* 375 Ma (23 and 19 analyses, respectively), and a subordinate age component composed of eight analyses at *c.* 365 Ma.

The oldest age group (*c.* 395 Ma) is present only in samples G07-1 and G07-2. It could be interpreted either as inheritance or as the age of the magmatic protolith. The absence of xenocrystic cores indicates that inheritance is absent in these samples and therefore proves this possibility wrong. Therefore, the ages around 395 Ma in these samples are interpreted as the crystallization age of the protolith. This interpretation is in agreement with their CL textures (oscillatory, sector and homogeneous zoning) and Th/U ratios (>0.1). Now that this approximate number has geological significance, we can use statistics to obtain an accurate age. In sample G07-1, 14 analyses yield a mean age of 395 ± 3 Ma, with a mean square of weighted deviation (MSWD) of 1.9 (Fig. 8a). In sample G07-2, nine analyses yield a mean age of 395 ± 2 Ma, with an MSWD of 0.92 (Fig. 8b). This age is older than the $^{40}Ar/^{39}Ar$ age obtained by Peucat *et al.* (1990) in an amphibole concentrate from a Grt-bearing amphibolite of the Purrido formation (391 ± 6.6 Ma), which probably represents a metamorphic age. A more similar age was obtained for the crystallization age of the magmatic protolith in the Careón ophiolite (395 ± 2 Ma, U–Pb TIMS on zircon; Díaz García *et al.* 1999) located in the adjacent Órdenes Complex.

The next age group (380–375 Ma) is present in samples G07-1, G07-2 and G07-7. In the last sample, the low Th/U ratios (between 0.01 and 0.13; Fig. 7) and the CL textures (sector and homogeneous luminescent zoning; group 3) suggest an episode of zircon growth during a metamorphic event. In contrast, most of the zircons from samples G07-1 and G07-2 yielding this age belong to group 1 and cores of group 2 (combined oscillatory and sector zoning). Furthermore, Th/U ratios in these samples are higher than 0.1, pointing to a magmatic rather than

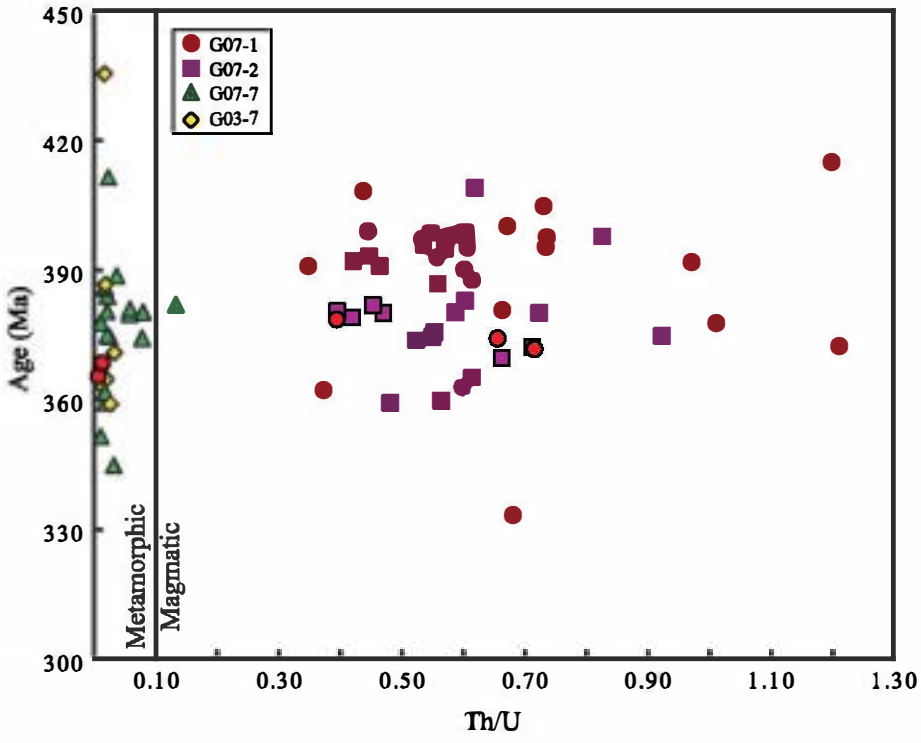

Fig. 7. Th/U ratio v. age diagram.

metamorphic origin for these zones. Consequently, we interpret that the metamorphic event registered in sample G07-7 triggered a lead loss episode in magmatic zircons from samples G07-1 and G07-2 (Fig. 8), but was not accompanied by new zircon growth. Metamorphic ages in the range 375–380 Ma have been already reported in an ophiolite from the Órdenes Complex (378.1 ± 0.4 Ma, ^{39}Ar–^{40}Ar age in amphibole concentrate; Dallmeyer *et al.* 1997).

Analyses from the youngest age component in these samples (*c.* 365 Ma) are less abundant, but they appear in all the samples. In sample G07-1, four analyses performed on zircons from groups 1, 2 (rim) and 3 yield a lower intercept age of 364 ± 5 Ma, anchored at $^{207}Pb/^{206}Pb = 0.860 \pm 0.001$, with an MSWD of 0.14 (Fig. 8a). In sample G07-2, a mean age of 365 ± 7 Ma is obtained from four analyses on group 1 zircons (Fig. 8b), with a high MSWD value (2.6). In sample G07-7, another four analyses yield a mean age of 360 ± 3 Ma, with an MSWD of 1.14 (Fig. 6a). This age group is probably related to continued lead loss during metamorphism either in magmatic (Th/U ratio >0.1) or metamorphic (Th/U ratio <0.1) zircon grains. Dallmeyer *et al.* (1991, 1997) reported similar ages in the Morais, Órdenes and Cabo Ortegal complexes (^{39}Ar–^{40}Ar ages on muscovite and whole-rock concentrates from greenschist-facies rocks).

LA-ICP-MS geochronology: sample description and results

The amphibolite sample G03-8 collected from the most representative outcrop of this mafic unit, located at the Purrido Mount quarry, was previously dated by LA-ICP-MS (U–Pb on zircon grains) at the Natural History Museum of London. The results obtained, corresponding to the analysis of 21 zircon grains, were discussed in detail by Sánchez Martínez *et al.* (2006), and the age for the main population (10 analyses) was interpreted as the crystallization age of the rock at *c.* 1160 Ma. Furthermore, this sample contained minor populations with ages in the range of 1.2–1.6 Ga and 322–428 Ma, and a single analysis of *c.* 800 Ma. Taking into account the contrasting results obtained in the rest of samples analysed by SHRIMP and that the geochronology of this sample itself was complex, we considered it necessary to further study sample G03-8 to better constrain the timing of the possible events recorded in the evolution of this apparently singular rock.

Thirty-three new analyses were performed on 21 zircon grains of the amphibolite sample G03-8 (see Fig. 9), four of which had not been analysed during the previous study of Sánchez Martínez *et al.* (2006). Twenty of the obtained analyses are concordant (90–110% concordance) whereas the rest have variable degree of discordance, defining a collinear array (Fig. 10a) whose meaning will be discussed below. According to their apparent age, it is possible to distinguish three groups of analyses.

The main group comprises 12 concordant or sub-concordant analyses (82–104% concordance) corresponding to eight zircon grains whose $^{207}Pb/^{206}Pb$ age ranges between 1084 ± 62 and 1198 ± 49 Ma (Fig. 10a and b). Most of these analyses correspond to zircons with typical oscillatory zoning characteristic of magmatic crystals. More discordant analyses were acquired from domains with a faded zoning that could explain a certain disturbance of the isotopic ratio. Generally they have Th/U ratios higher than 0.1, which also is indicative of an igneous origin. This group of data yielded an upper intercept of 1155 ± 14 Ma corresponding to a discordia line (Fig. 10b) with its lower intercept at 227 ± 150 Ma (MSWD = 1.2). The age of the upper intercept is equivalent to that corresponding to the median value of the $^{207}Pb/^{206}Pb$ ages of 10 analyses of these same zircons (1159 ± 39 Ma) published by Sánchez Martínez *et al.* (2006), which was formerly interpreted as the crystallization age of the rock. There are seven variably discordant analyses (49–88% concordance) with lower apparent Pb–Pb ages, which are distributed along a discordia line that has an upper intercept at *c.*

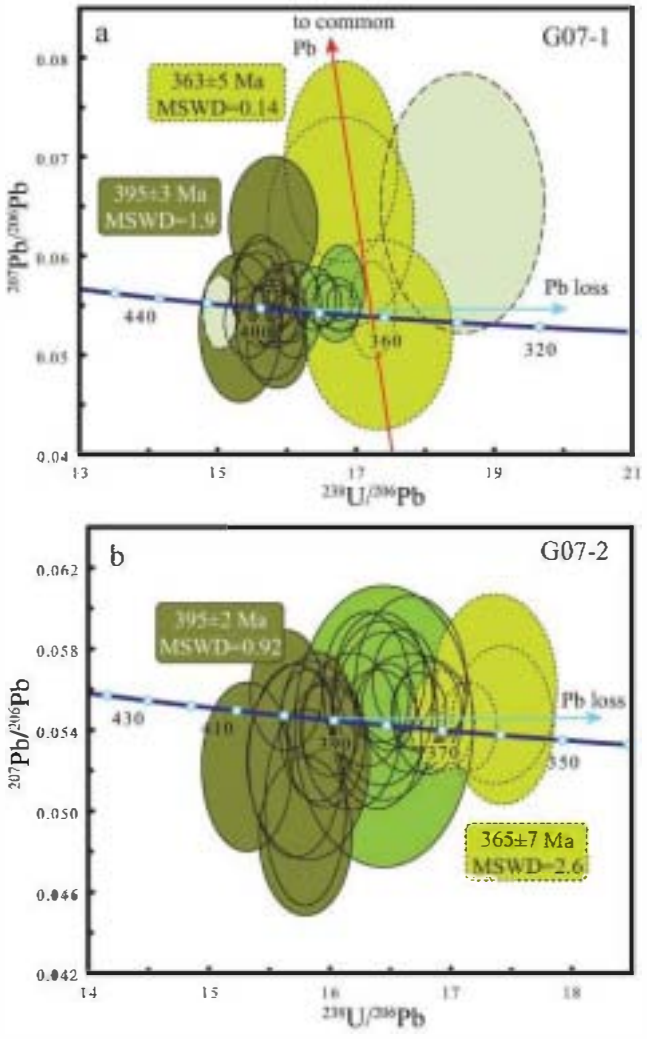

Fig. 8. Tera Wasserburg plot showing SHRIMP zircon analyses from samples (a) G07-1 and (b) G07-2. Olive green filled ellipses represent protolith magmatic ages; continuous-line blue green filled ellipses represent lead loss ages equivalent to metamorphic ages in sample G07-7. Dotted-line ellipses represent lead loss ages similar to sample G03-7. Dashed-line ellipses were not considered for the calculation of the former ages. Error ellipses are $\pm 2\sigma$.

1.1 Ga. Most of them show Th/U < 0.1, which generally indicates a metamorphic origin. The CL images reveal that these analyses were performed on structureless thin rims overgrowing oscillatory zoned magmatic cores (Mesoproterozoic in age) and on homogeneous domains without noticeable zoning or domains with blurred zoning. When calculating a discordia line including both the group of discordant analyses and the main Mesoproterozoic group of data, the upper and lower intercepts that we obtain for it are 1160 ± 24 and 295 ± 84 Ma (MSWD $= 3.0$) respectively (Fig. 10a); this is within the error range of the discordia calculated with only the main population. The relationship between these groups of data will be discussed below in the light of the zircon Lu–Hf isotope compositions. A final point to be considered is that some of the analyses could have developed a certain degree of Pb loss at present, which would slightly affect their concordance or alignment along the discordia lines.

The second group of analyses yield apparent $^{207}Pb/^{206}Pb$ ages ranging from 1230 ± 25 to 1605 ± 41 Ma, corresponding to five zircon grains (Fig. 10c). The concordant analyses correspond to domains with oscillatory zoning, suggesting a magmatic origin. Those that are discordant do not seem to be related to the discordant analyses of the first group or to the discordia line yielding an upper intercept at 1100 Ma. It is difficult to ascertain if these zircons all have the same origin, or if they represent different ages. The first possibility implies that all were older than the main group (around 1500–1600 Ma) and they were variably affected by the thermal event corresponding to the crystallization of the Mesoproterozoic zircons. If so, their concordia ages would be apparent and they would represent a discordia with a lower intercept at *c.* 1.1 Ga, which would be difficult to distinguish from the concordia itself because of their similar slope at these ages. Another possibility is that the different zircons crystallized at different ages and represent different inherited populations; this is an interpretation that will be further discussed in the light of the zircon Hf isotope data. However, it seems that these older grains would also have been affected by the same thermal event that affected the younger Mesoproterozoic zircons (lower intercept of the discordia line in Fig. 10a), considering that their most discordant analyses appear to be aligned according to a discordia line with a lower intercept at 556 ± 270 Ma (Fig. 10c), which overlaps within error the discordia line obtained for the main group of analyses.

Finally, there is a group of four concordant or sub-concordant analyses (86–126% concordance) corresponding to three zircon grains that yielded notably younger $^{206}Pb/^{238}U$ ages in the range of 397 ± 10 to 439 ± 9 Ma (Fig. 10d). Taking into account the resemblance of these ages to those obtained for the lower intercept given by the discordia line of the main group of analyses, a relationship between these datasets is permissible. However, considering only U–Pb geochemistry of these zircons we cannot rule out that these younger grains were formed in another, younger magmatic event. In this scenario, these zircon grains could be equivalent to the Devonian zircons dated in G07-1 and G07-2 and interpreted as dating the protolith age for these metagabbros. Unfortunately, the CL images corresponding to these three young zircons are not clear enough for us to say whether they could be igneous or metamorphic, but a high Th/U (0.31–0.57) suggests an igneous origin.

Lu–Hf zircon isotope geochemistry (LA-MC-ICP-MS)

Hafnium isotope measurements on zircons corresponding to samples G03-8, G07-1 and G07-2 were performed with a ThermoScientific Neptune multicollector (MS) ICP-MS system at Goethe University of Frankfurt coupled to the same laser ablation system and cell as described for the U–Pb analyses of sample G03-8, following the analytical procedures described by Gerdes & Zeh (2006, 2009) and Zeh *et al.* (2007*a*,*b*).

Lu–Hf isotope results

Twenty-one analyses were performed on zircon domains previously analysed for U–Pb determination corresponding to sample G03-8, from which it is possible to distinguish a main group (12 analyses) including both concordant and discordant analyses with similar $^{176}Hf/^{177}Hf_{int}$ (average value of 0.28216 ± 0.00004, ± 1SD, Fig. 11a). The concordant analyses correspond to the zircons dated at *c.* 1100 Ma and the discordant analyses are those that were considered to define a discordia connected with the Mesoproterozoic analyses, thus their $^{176}Hf/^{177}Hf_{int}$ ratio confirms the existence of a genetic

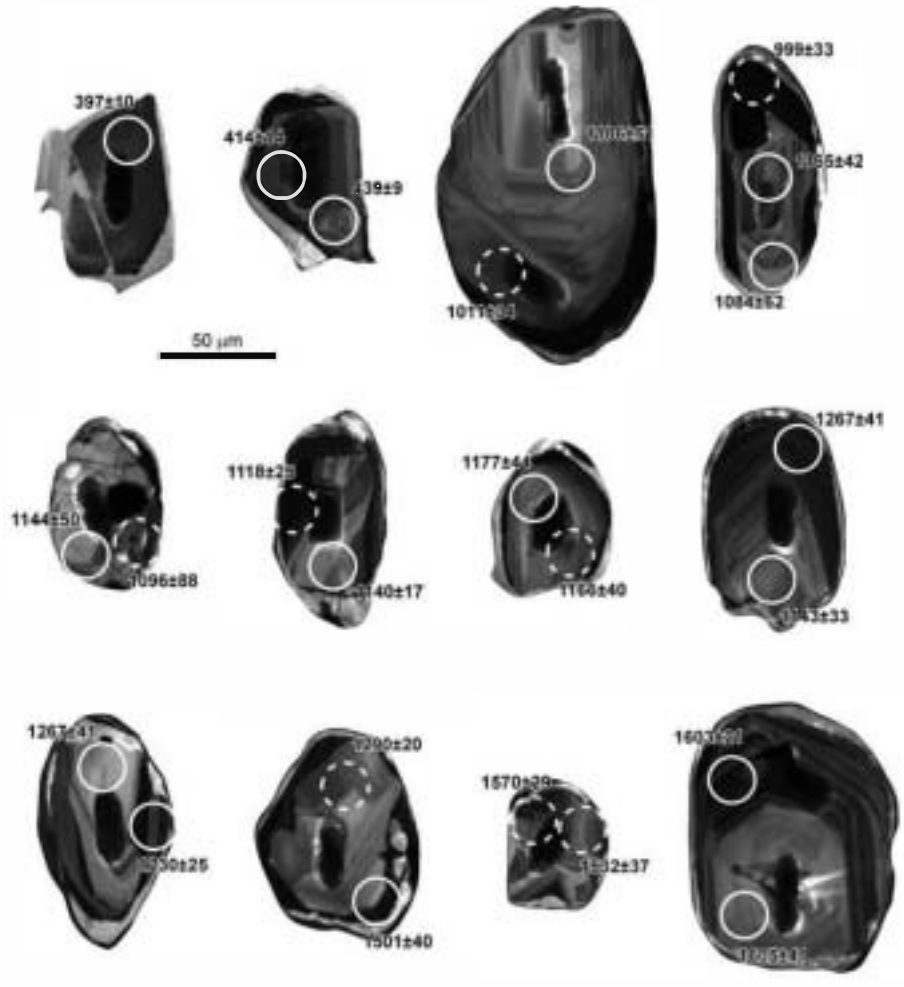

Fig. 9. Cathodoluminescence images of selected zircons from sample G03-8. The spot size represented by circles is 20 μm. Continuous-line circles correspond to concordant U–Pb determinations and dashed-line circles to discordant analyses.

relationship between them. Regarding their $^{176}Lu/^{177}Hf$ ratios, they display a larger variation, which suggests a certain degree of fractional crystallization. There is also a minor group of analyses that show lower $^{176}Hf/^{177}Hf_{int}$ ratios corresponding to the zircon domains that yielded Pb–Pb ages between 1230 and 1605 Ma (both concordant and discordant). Four of them are within the same range in their isotopic composition although the other two have ratios that are intermediate between these and the main Mesoproterozoic analyses. Finally, there are only two analyses corresponding to the youngest crystals present in this rock (*c.* 400 Ma), which have much higher $^{176}Hf/^{177}Hf_{int}$ ratios compared with the main group (Fig. 11a). It is clear that, according to these data, the two groups of zircons (older and younger) are not genetically connected, and thus grew during separate crystallization events. This separate origin is also reflected in the εHf v. age diagram, where it is possible to observe that these two zircons have εHf values higher and more primitive than those corresponding to the Mesoproterozoic analyses (Fig. 11b). Furthermore, this diagram indicates that whereas the main group of concordant zircon domains yielding *c.* 1.1 Ga still preserve their Pb–Pb age and Hf-isotope information unperturbed, those domains that yielded discordant analyses with younger apparent ages have been affected by lead loss via alteration during a later thermal event. Their U–Pb system has been reset whereas their Hf isotope system was unaffected (see Zeh *et al.* 2007*a*,*b*, 2009; Gerdes & Zeh 2009). Thus they have evolved along a $^{176}Lu/^{177}Hf = 0$ trend giving the lowest εHf values (−9.2 to −10.7). If their εHf were calculated for their 'true age' (i.e. 1100 Ma) their values would be within the same range as the concordant analyses (1.5–3.6), which is consistent with derivation from the same source and coeval crystallization.

In the zircons belonging to samples G07-1 and G07-2, 21 and 20 analyses were performed respectively in the same domains where the U–Pb determinations were acquired by SHRIMP. Except for three analyses from sample G07-1 the zircons have a very homogeneous $^{176}Hf/^{177}Hf_{int}$ ratio, with an average of 0.28287 and a scatter of only ±0.00003 (1SD), which approximately corresponds to 2 εHf units. These ratios are much higher than the $^{176}Hf/^{177}Hf_{int}$ ratios of the Mesoproterozoic zircons of sample G03-8 but are within the range for the two Devonian zircons found in that sample (Fig. 11a). As has been pointed out, only three analyses corresponding to sample G07-1 have slightly lower ratios. Both samples display a wider range of $^{176}Lu/^{177}Hf$ values, which can be explained either by fractional crystallization processes or by later metamorphism, relative to the younger analyses, although a clear correlation between $^{176}Lu/^{177}Hf$ and Th/U ratios is not observed and the real meaning is not clear. With the exception of the three analyses previously mentioned, the other zircons have strongly positive εHf values (10–14) overlapping with the depleted mantle evolution array calculated for mid-ocean ridge

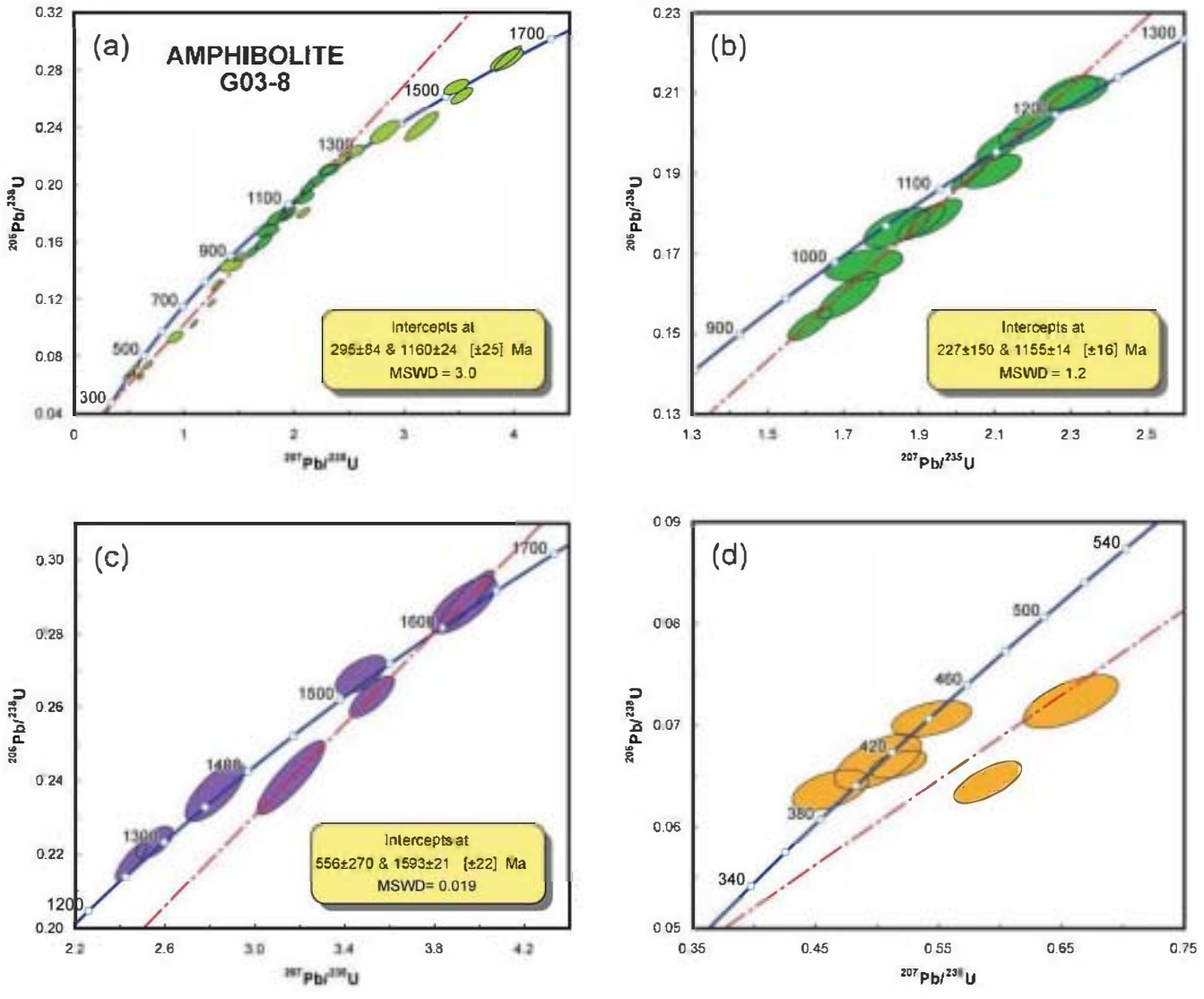

Fig. 10. Complete (a) and partial (b–d) concordia plots showing distribution of LA-ICP-MS zircon analyses from sample G03-8. Groups of analyses have been represented in different colours. Error ellipses are 2σ.

basalts (MORB) (Fig. 11b), implying that they correspond to zircons crystallized from a juvenile magma derived from a mantle source that was not modified by assimilation of older crust. Only two Devonian zircons belonging to sample G03-8 have εHf values similar to those of samples G07-1 and G07-2, and thus they should have the same origin, unlike the Mesoproterozoic zircons. On the other hand, the possible explanation that justifies the occurrence of the three Devonian analyses in sample G07-1 with lower εHf (6.4–8.3) is that, although they represent newly grown zircons, they record a certain degree of contamination with the older component represented by the Mesoproterozoic zircons. These Mesoproterozoic crystals have positive εHf values ranging between 1.5 and 3.6 for the main group with *c.* 1.1 Ga ages, and between 0.7 and 4.3 for those with older Pb–Pb ages. Although all are still primitive according to these positive values, they are not as close to the depleted mantle values as the Devonian grains are, which implies that they reflect some extent of mixture of the mantle source with an older or crustal component.

Interpretation of the Lu–Hf isotope results

According to the Lu–Hf isotope data, at least two major zircon-forming events can be identified in the Purrido unit: the older has a Mesoproterozoic age and the youngest occurred during Devonian times. The sources from which these groups of zircons derive are different. The magma from which the Devonian zircons crystallized is juvenile, with an isotopic composition resembling that of the depleted mantle. The Mesoproterozoic zircons derive from a magma slightly contaminated with a crustal or older component, which can be justified by the presence of a minor population of zircons older than *c.* 1.1 Ga. The variation of the $^{176}Lu/^{177}Hf$ ratios in both groups of Devonian and Mesoproterozoic zircons indicates the occurrence of fractional crystallization processes during the genesis of these rocks. A few Mesoproterozoic zircons underwent Pb loss during a subsequent thermal event but preserve their $^{176}Hf/^{177}Hf_{int}$. Considering that they form part of a discordia line with a lower intercept close to 400 Ma, the most plausible interpretation is that this would be the age of that event.

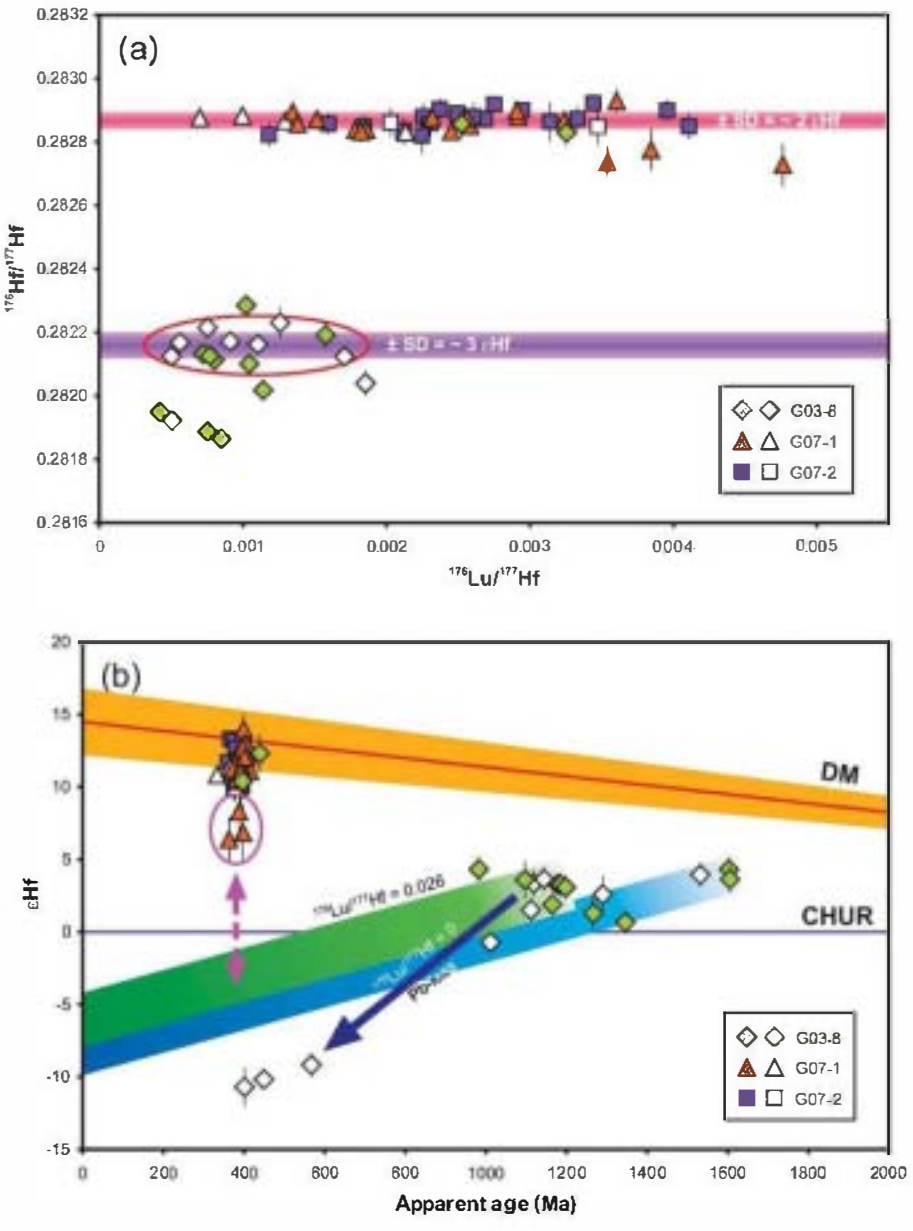

Fig. 11. Plots of initial $^{176}Hf/^{177}Hf$ v. $^{176}Lu/^{177}Hf$ (a) and εHf v. apparent age (b) showing the results of Lu–Hf spot analyses of zircons from samples G03-8, G07-1 and G07-2. Filled symbols correspond to concordant U–Pb analyses; open symbols are discordant. Error bars are 2σ. The horizontal coloured bands in (a) correspond to the average $^{176}Hf/^{177}Hf_{int}$ values for the main groups of analyses represented with ±1 SD. Parameters used for the calculation of initial εHf plotted in (b) are defined in the text. The depleted mantle array (DM) is extrapolated from average present-day values of MORB (Chauvel & Blichert-Toft 2001), assuming a linear behaviour from $\varepsilon Hf = 2$ at 4000 Ma (Vervoort & Blichert-Toft 1999). The oblique overlapping coloured bands represent $\varepsilon Hf(t)$ bulk-rock evolution trends calculated using $^{176}Lu/^{177}Hf$ of 0.026 representative for MORB (Blichert-Toft & Albarède 2008). The blue arrow represents a Pb-loss trend followed by some of the old zircon domains. The vertical double-headed arrow defines a possible mixing line between the juvenile source and a Mesoproterozoic component at *c.* 400 Ma, which affected the three encircled analyses of sample G07-1.

There are only three analyses of *c.* 400 Ma zircons that suggest certain interaction between the juvenile magma and the Mesoproterozoic component (pink double-headed arrow in Fig. 11b). These analyses can be explained only by accepting some contamination of the juvenile Devonian magma with an older Mesoproterozoic source. In any case, the Hf isotope systematics in these zircons shows that this interaction and contamination was rather limited, at least in relation to the chemistry of zircon. The interaction of the Devonian juvenile magma with the Mesoproterozoic component was not important enough to cause the re-equilibration of the Hf isotope system of this old component.

Sm–Nd whole-rock isotope geochemistry

Sm–Nd isotope determinations were performed on 17 common amphibolites from the Purrido unit (samples CE-14 to CE-31). These are the same samples as investigated by Sánchez Martínez *et al.* (2007*b*) for major and trace element geochemistry, and also the samples used in the trace element diagrams presented in Figure 4. The sample localities are shown in Figure 3. A small remnant volume of sample G03-8 investigated for U–Pb geochronology on zircon (a fragment of several grams from the original sample of 10 kg used for zircon separation) was also analysed for Sm–Nd isotope geochemistry. The Sm–Nd analyses were performed using a multicollector Finnigan Mat 262 mass spectrometer in static mode at the Memorial University of Newfoundland.

Sm–Nd results

The investigated metabasites from the Purrido unit taken all together show a large variation in their Sm–Nd compositions, with $^{147}Sm/^{144}Nd$ ratio ranging from 0.1622 to 0.2193 and $\varepsilon Nd(0)$ ranging from +5.9 to +9.9 (Fig. 12a and b). This Nd isotopic heterogeneity is also observed at any of the obtained U–Pb ages (with $\varepsilon Nd(t)$ values ranging from +7.5 to +9.3 at 400 Ma and +6.1 to +11.2 at 1100 Ma). Furthermore, it can be

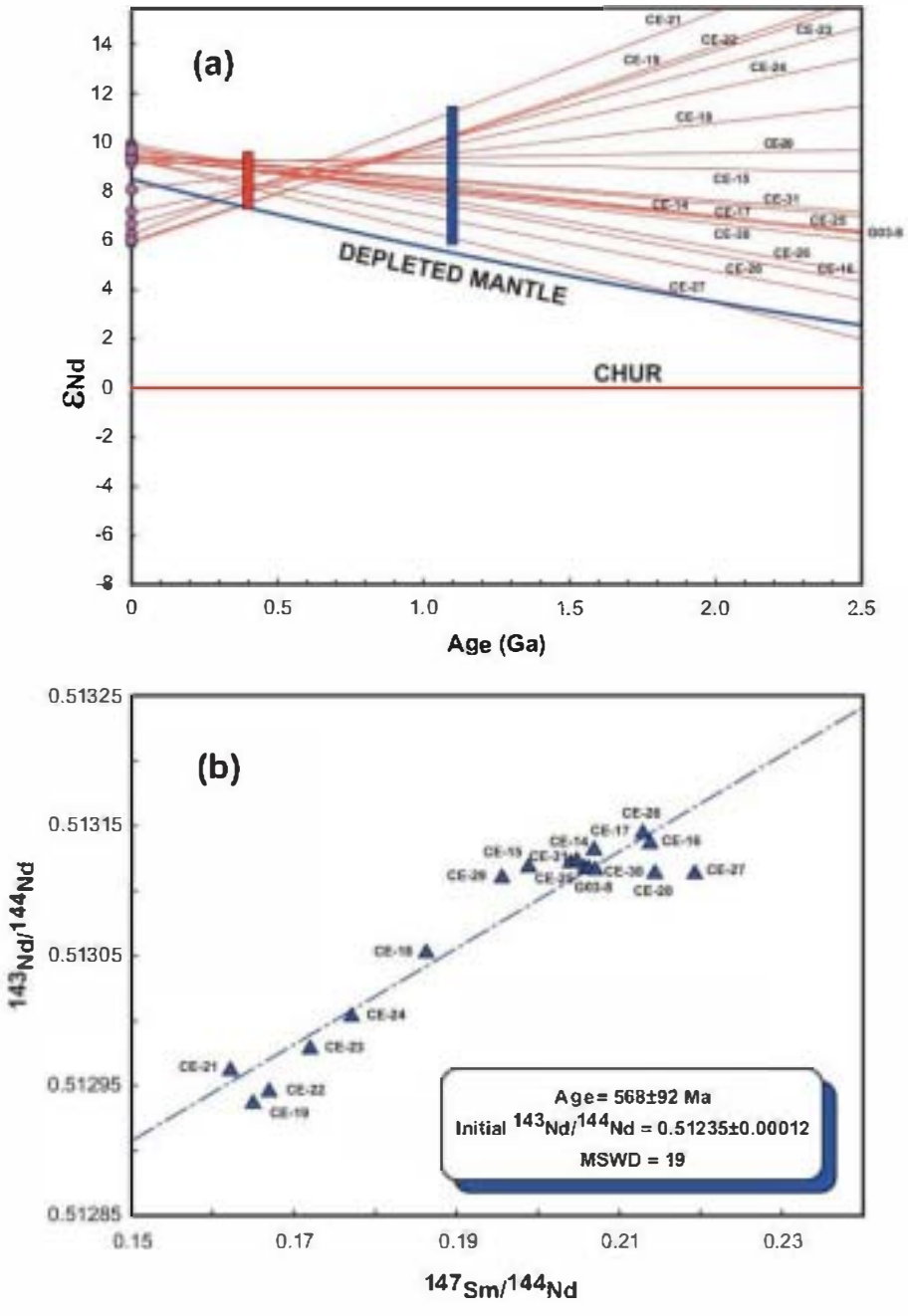

Fig. 12. (a) εNd v. age (Ga) diagram showing the growth lines of 18 selected amphibolites of the Purrido unit. The red and blue bars show the εNd range at 400 and 1100 Ma respectively. Depleted mantle line after DePaolo (1981). (b) Sm–Nd isotopic correlation diagram for whole-rock analyses of the 18 amphibolite samples from the Purrido unit.

seen in Figure 12a that the samples do not represent a coherent ensemble but seem to define two groups, the main one comprising 12 samples with Nd evolution lines subparallel to the Depleted Mantle evolution and characterized by positive $f_{Sm/Nd}$ values ($^{147}Sm/^{144}Nd$ ratios > 0.1967). The second group comprises six samples showing more crustal-like evolution characterized by negative $f_{Sm/Nd}$ values ($^{147}Sm/^{144}Nd$ ratios < 0.1967) (Fig. 12). Samples CE-15 and CE-29 show intermediate compositions between the two groups. In any case, the εNd v. time diagram provides only limited information about the geochronology of the Purrido amphibolites, where samples with zircon populations with different U–Pb ages exist. Most of the common mafic rocks show asymptotic trends with the depleted mantle evolution line, with little change with time. The samples with growth lines intersecting the depleted mantle at high angles are those with isotopic compositions less typical of common mafic rocks.

It is clear in Figure 12a that at least two sources were involved in the evolution of the Purrido amphibolites, on the basis of the high variation of the εNd values and the different trends exhibited by the growth lines of the two groups of samples. This conclusion is similar to that obtained with the Hf isotopic data, which also indicate the presence of two sources for the Purrido amphibolites. The existence of two groups of compositions is even more obvious when the samples are reported in a $^{143}Nd/^{144}Nd$ v. $^{147}Sm/^{144}Nd$ diagram, where the first group of 12 samples form a cluster that is parallel to the x-axis and very homogeneous with respect to their $^{143}Nd/^{144}Nd$ ratio (ranging

from 0.513112 to 0.513146 for their measured ratio, corresponding to a range of +8.2 to +9.3 for their εNd(400)), whereas samples from the second group scatter along a poorly defined correlation line (Fig. 12b). No correlation could be obtained using the 18 samples taken together, as indicated by a high MSWD value of 19 (Fig. 12b). However, if only the six samples of the second group are taken, a poorly constrained correlation at 677 ± 310 Ma (MSWD = 8.9) could be calculated.

Interpretation of the Sm–Nd results

The whole-rock Nd isotopic composition of the Purrido amphibolites clearly indicates a complex origin for the generation of these mafic rocks, as the large variation observed in both the $^{147}Sm/^{144}Nd$ and $^{143}Nd/^{144}Nd$ ratios of the samples cannot be interpreted as resulting only from the magmatic differentiation of a single magmatic source and ^{147}Sm decay. From the study of the Sm–Nd systematics, two groups of samples seem to emerge.

The first group is the most important in volume and is characterized by high Sm/Nd ratio ($f_{Sm/Nd} > 0$), higher Nd isotopic composition (εNd(400) ranging from +8.2 to +9.3) and sample evolution lines through time that are subparallel to that of the Depleted Mantle. These characteristics are similar to those typical of modern basaltic rocks with MORB compositions (DePaolo 1988) and hence we interpret this group as being representative of the Devonian gabbroic source. The metagabbroic samples forming a single population of magmatic zircons dated at *c.* 395–396 Ma and having juvenile Devonian Hf signatures would be part of this group.

The second group seems to be minor in volume and is characterized by low Sm/Nd ratio ($f_{Sm/Nd} < 0$) and lower Nd isotopic composition (with εNd(400) ranging from +7.5 to +8.2). The interpretation of this second group is less straightforward and depends on the interpretation of the possible regression lines in the isochron diagram. We interpret the Sm/Nd results obtained on the second group of samples as resulting from the mixing of a Devonian mantle-derived magma (represented by the first group of 10–12 samples) with a much older basement. However, the final interpretation of the Sm–Nd data is possible only in the context of a general discussion considering also the U–Pb and Lu–Hf data and will be addressed below.

Discussion

Chronology of the lithologies and sources involved in the Purrido unit

The initial U–Pb dating of the main zircon population in sample G03-8 at 1159 ± 39 Ma (Sánchez Martínez *et al.* 2006) led to the interpretation of the Purrido unit as a Mesoproterozoic ophiolite rarely preserved in the Variscan suture. The data presented in this paper allow us to review the meaning of this unit and to offer a different interpretation for its origin. Two samples of amphibolites yielded populations of igneous zircons dated at 395 ± 3 Ma and 395 ± 2 Ma, samples G07-1 and G07-2 respectively (Fig. 8). These ages are interpreted as dating the emplacement of the protoliths of both samples, which can therefore be identified as Devonian metagabbros. Most of the zircons in both samples show Hf isotopic signatures similar to those of the depleted mantle at 400 Ma (Fig. 11b), which allows the identification of the gabbro protoliths as juvenile rocks generated after partial melting of a mantle source. In the same way, Sm–Nd results obtained on 12 of the 18 analysed whole-rock samples clearly indicate a juvenile mantle-derived origin for their magmatic protoliths with high Sm/Nd ratio ($f_{Sm/Nd} > 0$) and εNd(400) ranging from +8.2 to +9.3, in agreement with a direct derivation of the magmas from a Devonian Depleted Mantle (Fig. 12a).

Three of the samples dated by SHRIMP (G07-1, G07-2, G07-7) contain populations of metamorphic zircons with U–Pb ages ranging between 375 and 380 Ma (Figs 6 and 8). These ages are similar to others obtained by $^{39}Ar/^{40}Ar$ in ophiolites from the NW Iberian Massif, considered as related to the main event of deformation and metamorphism that affected these units (Dallmeyer *et al.* 1997). Therefore it is clear, according to the new data presented here, that the Purrido unit contains juvenile gabbros of Middle Devonian age that were later affected by deformation and metamorphism during the Late Devonian, probably during their incorporation into an accretionary complex.

This study has reviewed the U–Pb zircon geochronology in sample G03-8, which was first interpreted as a Mesoproterozoic metagabbro (Sánchez Martínez *et al.* 2006). The new data confirm the presence of a main zircon population with a refined chronology of 1155 ± 14 Ma and some older zircons with ages around 1500–1600 Ma (Fig. 10). Moreover, this sample includes three zircons with younger ages ranging between 397 ± 10 and 439 ± 9 Ma. The Hf isotope geochemistry shows that the Mesoproterozoic zircons are relatively juvenile (Fig. 11b), although their compositions suggest some contamination or mixing with an older source, probably represented by the oldest Mesoproterozoic zircons (1500–1600 Ma). The youngest zircons in this sample have juvenile character, with εHf_{int} values similar to those of the depleted mantle at 400 Ma, identical to those exhibited by the common Devonian igneous zircons in G07-1 and G07-2 (Fig. 11b). From a Sm–Nd point of view results obtained on this sample place it typically in the group of samples interpreted as classical Devonian gabbro with a positive $f_{Sm/Nd}$ of +0.05 and an εNd(400) of +8.9. A first interpretation of these data could suggest that sample G03-8 is a Devonian metagabbro that assimilated Mesoproterozoic material and preserves zircon xenocrysts from that source. However, the minor Devonian zircons present in this sample, as opposed to what is typical of samples G07-1 and G07-2 collected from the same Purrido Mount quarry, the high number of Mesoproterozoic zircons and Sm–Nd isotope composition more typical of the Devonian gabbros, are puzzling questions that require more detailed study before a final interpretation can be proposed.

Probably one of the most interesting features to consider is the presence in sample G07-1 of three Devonian zircons with compositions that suggest mixing of the juvenile Devonian gabbroic magma and the Mesoproterozoic source (Fig. 11b). These zircons suggest that the Devonian mafic magma assimilated older material, probably of Mesoproterozoic age according to the U–Pb dating of zircon in sample G03-8, and was contaminated to some extent. However, only three of the *c.* 40 analysed zircons show evidence for this contamination, which at first should be interpreted as an indication of a limited interaction, as the Hf isotope geochemistry on zircon easily traces mixing processes. In this regard it is important to underline that the youngest zircons in sample G03-8 do not show any evidence of crystallization from a magma contaminated with Mesoproterozoic material, even considering that the main zircon population in this sample has Mesoproterozoic age. This indicates that in relation to the Lu–Hf isotope geochemistry, the sources of the Devonian and Mesoproterozoic zircons do not show clear evidence of mixing in sample G03-8, which in this case should be considered an indication of separate zircon crystallization

events from different unmixed sources. As a whole, these data seem to indicate that mixing processes existed in the generation of the Devonian gabbros, but apparently they were of only limited extent with respect to the Lu–Hf on zircon systematics.

However, Sm–Nd results obtained on six of the 18 analysed whole-rock samples clearly indicate a significant interaction between the Devonian mantle-derived magma and an older component, most certainly a Mesoproterozoic basement. This apparent discrepancy between the extent of contamination observed in the Sm–Nd data on whole rock when compared with Lu–Hf on zircon suggests that the Mesoproterozoic zircons could have survived a Devonian assimilation process and thus preserved the Devonian magma from being contaminated by an older Hf component as most of the Hf is hosted by the zircon. In contrast, the Nd isotopic composition of the Devonian magma may have been more easily affected by a contamination process, as Nd in basic rocks is not hosted by any specific phase but instead is disseminated within the rock-forming minerals that will be assimilated during the contamination process. The development of extended mixing processes is largely favoured between contemporary magmas with a similar rheological behaviour (Sato *et al.* 2007; Kratzmann *et al.* 2009; Tonarini *et al.* 2009), but it is hindered where the interaction occurs between the magma and colder and/or older rocks. Another explanation could be that the remnants of the Mesoproterozoic basement in the Purrido unit are present only locally, either as xenoliths or as exotic lenses sheared within the Devonian gabbro, making their recognition extremely difficult in the field. In this context, some Purrido samples could represent a mechanical mixture of the two lithologies. The presence of this Mesoproterozoic basement in the unit could range from a limited extent, even at the scale of xenoliths in the Devonian gabbros, to a much larger presence. Probably future Lu–Hf whole-rock research may help to solve this question.

Ophiolite generation and interaction with a Mesoproterozoic basement

The Purrido unit was included in the upper ophiolites of the NW Iberian Massif (Arenas *et al.* 2007*a*; Sánchez Martínez *et al.* 2007*b*), although the recent discovery of lithologies with Mesoproterozoic age has changed this initial classification (Sánchez Martínez *et al.* 2006, 2009). At present, the new discovery of Devonian gabbros allows us to relate again this unit with other mafic–ultramafic sequences dated at 395 Ma, as is the case of the Careón ophiolite in Galicia (Díaz García *et al.* 1999; Pin *et al.* 2002; Sánchez Martínez *et al.* 2007*a*). The Devonian ophiolites are probably the most common oceanic type in the Variscan suture, as their presence is also well known in other parts of the Variscan Belt. This group of ophiolites also includes, for instance, the Lizard ophiolite of Cornwall (Clark *et al.* 1998; Nutman *et al.* 2001) and the Ślęża ophiolite in the Bohemian Massif (Oliver *et al.* 1993; Dubińska *et al.* 2004; Kryza & Pin 2010). These are suprasubduction-zone ophiolites generated in tectonic settings characterized by major extension, as is suggested by the presence of diabase dykes intruding any level of the succession, including the mantle section. In the NW of the Iberian Massif, these mafic rocks show typical compositions of island-arc tholeiites, and they have been interpreted as generated in an intra-oceanic subduction environment. This subduction would remove the old and cold lithosphere of the Rheic Ocean, and this region would be the most important destructive plate margin during the closure of the ocean; that is, the zone where most of the common N-MORB oceanic rocks disappeared (Sánchez Martínez *et al.* 2007*a*).

The data presented in this paper provide evidence of interaction between Devonian gabbros and a Mesoproterozoic mafic basement. If such interaction did occur, the Devonian gabbros intruded much older rocks whose presence is not compatible with magmatism in a large intra-oceanic subduction zone. If it is accepted that this supposed intra-Rheic subduction zone dipped to the north (Sánchez Martínez *et al.* 2007*a*; Gómez Barreiro *et al.* 2010), the most probable location for this basement would have been along the northern margin of Gondwana and would have arrived at the subduction zone by Middle Devonian times, where it interacted with the area of generation of the mafic magmatism, in the context of a hitherto poorly understood palaeogeographical setting. The Mesoproterozoic zircon populations identified in the amphibolites are not compatible with derivation from the West African Craton, but they could be correlated with the Saharan Craton or the Arabian–Nubian Shield. This basement could be the same domain that has been considered as a possible primary source for the detrital zircon populations with Mesoproterozoic ages in Palaeozoic sedimentary rocks both in the Central Iberian Zone and in the basal units of the allochthonous complexes (see Díez Fernández *et al.* 2010, and references therein). However, detrital zircon populations in Palaeozoic sedimentary rocks show less than 20% of Mesoproterozoic zircons, and are dominated by zircon populations with Neoproterozoic or Palaeozoic ages. The basement involved in the Purrido unit should be represented by Mesoproterozoic mafic rocks derived from the peri-Gondwanan lower continental crust, as a typical mafic composition is characteristic in all the lithologies from the Purrido unit. This Mesoproterozoic basement would have been intruded by the Devonian gabbros, developing some mixing processes to an unknown extent, and it may occur currently sheared among these gabbros in the Variscan suture zone preserved in the Cabo Ortegal complex.

Conclusions

(1) The Purrido unit contains metagabbros dated at 395 Ma, affected by a tectonothermal event at 375–380 Ma (zircon U–Pb, SHRIMP). The Purrido unit should be included within the upper ophiolitic units of the NW Iberian Massif.

(2) Although the unit cannot be considered a Mesoproterozoic ophiolite, as it was previously classified, the new zircon U–Pb geochronology, Lu–Hf (zircon) and Sm–Nd (whole-rock) isotope data prove that the Devonian gabbros intruded a Mesoproterozoic basement and developed, to some extent, assimilation and mixing processes with mafic rocks from this basement.

(3) As is suggested by the U–Pb dating of the dominant zircon population in sample G03-8 at 1155 ± 14 Ma (LA-ICP-MS), this basement may be preserved in the unit sheared among Devonian gabbros in the Variscan suture. However, the regional extent of this basement is unknown.

(4) The data presented in this paper are hard to reconcile with the generation of the most common ophiolites preserved in the Variscan suture in the setting of a normal intra-oceanic subduction zone. This conclusion provides new perspectives for Palaeozoic palaeogeography during the final stages of the closure of the Rheic Ocean.

We would like to thank the SUMAC staff at Stanford University, especially J. Wooden, for their help in operating the SHRIMP instrument and in interpreting the results. The stay by P. Castiñeiras at the SUMAC facility was financed with a 'Profesores UCM en el extranjero' travel aid.

S. Sánchez Martínez also thanks to the Spanish Ministerio de Ciencia e Innovación, which provided her with a 2 year post-doctoral contract to Goethe Universität Frankfurt am Main. Thanks also go to G. Brey for kindly hosting and welcoming at the Department of Mineralogy and Petrology of GUF. B. Murphy and J. Payne are gratefully acknowledged for insightful reviews of the paper. Financial support for this research has been provided by Spanish project CGL2007-65338-CO2-01/BTE (Ministerio de Ciencia e Innovación).

References

Abati, J., Castiñeiras, P., Arenas, R., Fernández-Suárez, J., Gómez-Barreiro, J. & Wooden, J. 2007. Using SHRIMP zircon dating to unravel tectonothermal events in arc environments. The early Palaeozoic arc of NW Iberia revisited. *Terra Nova*, 19, 432–439.

Arenas, R., Gil Ibarguchi, J.I., *et al.* 1986. Tectonostratigraphic units in the complexes with mafic and related rocks of the NW of the Iberian Massif. *Hercynica*, 2, 87–110.

Arenas, R., Martínez Catalán, J.R., *et al.* 2007*a*. Paleozoic ophiolites in the Variscan suture of Galicia (northwest Spain): distribution, characteristics and meaning. *In:* Hatcher, R.D., Jr, Carlson, M.P., McBride, J.H. & Martínez Catalán, J.R. (eds) *4-D Framework of Continental Crust*. Geological Society of America, Memoirs, **200**, 425–444.

Arenas, R., Martínez Catalán, J.R., Sánchez Martínez, S., Fernández-Suárez, J., Andonaegui, P., Pearce, J.A. & Corfu, F. 2007*b*. The Vila de Cruces Ophiolite: A remnant of the Early Rheic Ocean in the Variscan suture of Galicia (Northwest Iberian Massif). *Journal of Geology*, 115, 129–148.

Arenas, R., Sánchez Martínez, S., Castiñeiras, P., Jeffries, T.E., Díez Fernández, R. & Andonaegui, P. 2009. The basal tectonic mélange of the Cabo Ortegal Complex (NW Iberian Massif): a key unit in the suture of Pangea. *Journal of Iberian Geology*, 35, 85–125.

Azcárraga, J. 2000. *Evolución tectónica y metamórfica de los mantos inferiores de grado alto y alta presión del Complejo de Cabo Ortega*. Nova Terra, 17.

Blichert-Toft, J. & Albarède, F. 2008. Hafnium isotopes in Jack Hills zircons and the formation of the Hadean crust. *Earth and Planetary Science Letters*, 265, 686–702.

Chauvel, C. & Blichert-Toft, J. 2001. A hafnium isotope and trace element perspective on melting of the depleted mantle. *Earth and Planetary Science Letters*, 190, 137–151.

Clark, A.H., Scott, D.J., Sandeman, H.A., Bromley, A.V. & Farrar, E. 1998. Siegenian generation of the Lizard ophiolite: U–Pb zircon age data for plagiogranite, Porthkerries, Cornwall. *Journal of the Geological Society, London*, 155, 595–598.

Corfu, F., Hanchar, J.M., Hoskin, P.W.O. & Kinny, P. 2003. Atlas of zircon textures. *In:* Hanchar, J.M. & Hoskin, P.W.O. (eds) *Zircon*. Mineralogical Society of America and Geochemical Society, Reviews in Mineralogy and Geochemistry, 53, 468–500.

Dallmeyer, R.D., Ribeiro, A. & Marques, E 1991. Polyphase Variscan emplacement of exotic terranes (Morais and Bragança Massifs) onto Iberian successions: Evidence from $^{40}Ar/^{39}Ar$ mineral ages. *Lithos*, 27, 133–144.

Dallmeyer, R.D., Martínez Catalán, J.R., *et al.* 1997. Diachronous Variscan tectonothermal activity in the NW Iberian Massif: evidence from $^{40}Ar/^{39}Ar$ dating of regional fabrics. *Tectonophysics*, 277, 307–337.

DePaolo, D.J. 1981. Neodymium isotopes in the Colorado Front range and crust–mantle evolution in the Proterozoic. *Nature*, 291, 193–196.

DePaolo, D.J. 1988. *Neodymium Isotope Geochemistry*. Springer, Berlin.

Díaz García, F., Arenas, R., Martínez Catalán, J.R., González del Tánago, J. & Dunning, G.R. 1999. Tectonic evolution of the Careón Ophiolite (northwest Spain): a remnant of oceanic lithosphere in the Variscan Belt. *Journal of Geology*, 107, 587–605.

Díaz García, F., Sánchez Martínez, S., Castiñeiras, P., Fuenlabrada, J.M. & Arenas, R. 2010. A peri-Gondwanan arc in NW Iberia. II: Assessment of the intra-arc tectonothermal evolution through U–Pb SHRIMP dating of mafic dykes. *Gondwana Research*, 17, 352–362.

Díez Fernández, R., Martínez Catalán, J.R., Gerdes, A., Abati, J., Arenas, R. & Fernández-Suárez, J. 2010. U–Pb ages of detrital zircons from the Basal allochthonous units of NW Iberia: Provenance and paleoposition on the northern margin of Gondwana during the Neoproterozoic and Paleozoic. *Gondwana Research*, 18, 385–399.

Dubińska, E., Bylina, P., Kozłowski, A., Dörr, W. & Nejbert, K. 2004. U–Pb dating of serpentinization: Hydrothermal zircon from a metasomatic rodingite shell (Sudetic ophiolite, SW Poland). *Chemical Geology*, 203, 183–203.

Fisher, D. & Gerdes, A. 2009. Precise and accurate *in situ* U–Pb dating of zircon with high sample throughput by automated LA-SF-ICP-MS. *Chemical Geology*, 261, 261–270.

Fuenlabrada, J.M., Arenas, R., Sánchez Martínez, S., Díaz García, F. & Castiñeiras, P. 2010. A peri-Gondwana arc in NW Iberia. I: Isotopic and geochemical constraints on the origin of the arc—a sedimentary approach. *Gondwana Research*, 17, 338–351.

Gerdes, A. & Zeh, A. 2006. Combined U–Pb and Hf isotope LA-(MC)ICP-MS analyses of detrital zircons: comparison with SHRIMP and new constraints for the provenance and age of an Armorican metasediment in Central Germany. *Earth and Planetary Science Letters*, 249, 47–61.

Gerdes, A. & Zeh, A. 2009. Zircon formation versus zircon alteration—new insights from combined U–Pb and Lu–Hf *in-situ* LA-ICP-MS analyses, and consequences for the interpretation of Archean zircon from the Central Zone of the Limpopo Belt. *Chemical Geology*, 261, 230–243.

Gómez Barreiro, J., Martínez Catalán, *et al.* 2010. Fabric development in a Middle Devonian intra-oceanic subduction regime: the Careón ophiolite (NW Spain). *Journal of Geology*, 118, 163–186.

Kratzmann, D.J., Carey, S., Scasso, R. & Naranjo, J.A. 2009. Compositional variations and magma mixing in the 1991 eruptions of Hudson volcano, Chile. *Bulletin of Volcanology*, 71, 419–439.

Kryza, R. & Pin, C. 2010. The Central-Sudetic ophiolites (SW Poland): Petrogenetic issues, geochronology and palaeotectonic implications. *Gondwana Research*, 17, 292–305.

Ludwig, K.R. 2003. *ISOPLOT/Ex, version 3, A Geochronological Toolkit for Microsoft Excel*. Berkeley Geochronology Center Special Publication, 4.

Martínez Catalán, J.R., Arenas, R., *et al.* 2007. Space and time in the tectonic evolution of the northwestern Iberian Massif: Implications for the Variscan belt. *In:* Hatcher, R.D., Jr, Carlson, M.P., McBride, J.H. & Martínez Catalán, J.R. (eds) *4-D Framework of Continental Crust*. Geological Society of America, Memoirs, 200, 403–423.

Martínez Catalán, J.R., Arenas, R., *et al.* 2009. A rootless suture and the loss of the roots of a mountain chain: The Variscan belt of NW Iberia. *Comptes Rendus Géoscience*, 341, 114–126.

Matte, Ph. 1991. Accretionary history and crustal evolution of the Variscan belt in Western Europe. *Tectonophysics*, 196, 309–337.

Murphy, J.B. & Gutiérrez-Alonso, G. 2008. The origin of the Variscan upper allochthons in the Ortegal Complex, northwestern Iberia: Sm–Nd isotopic constraints on the closure of the Rheic Ocean. *Canadian Journal of Earth Science*, 4, 651–668.

Murphy, J.B., Gutiérrez-Alonso, G., *et al.* 2006. Origin of the Rheic Ocean: rifting along a Neoproterozoic suture? *Geology*, 34, 325–328.

Murphy, J.B., Gutiérrez-Alonso, G., Fernández-Suárez, J. & Braid, J.A. 2008. Probing crustal and mantle lithosphere origin through Ordovician volcanic rocks along the Iberian passive margin of Gondwana. *Tectonophysics*, 461, 166–180.

Nance, R.D., Gutiérrez-Alonso, G., *et al.* 2010. Evolution of the Rheic Ocean. *Gondwana Research*, 17, 194–222.

Nutman, A.P., Green, D.H., Cook, C.A., Styles, M.T. & Holdsworth, R.E. 2001. SHRIMP U–Pb zircon dating of the exhumation of the Lizard Peridotite and its emplacement over crustal rocks: Constraints for tectonic models. *Journal of the Geological Society, London*, 158, 809–820.

Oliver, G.J.H., Corfu, F. & Krough, T.E. 1993. U–Pb ages from SW Poland: Evidence for a Caledonian suture zone between Baltica and Gondwana. *Journal of the Geological Society, London*, 158, 809–820.

Pearce, J.A. 1996. A user's guide to basalt discrimination diagrams. *In:* Wyman, D.A. (ed.) *Trace Element Geochemistry of Volcanic Rocks: Application for Massive Sulphide Exploration*. Short Course Notes, Geological Association of Canada, 12, 79–113.

Peucat, J.J., Bernard-Griffiths, J., Gil Ibarguchi, J.I., Dallmeyer, R.D., Menot, R.P., Cornichet, J. & Iglesias Ponce de León, M. 1990. Geochemical and geochronological cross section of the deep Variscan crust: The Cabo Ortegal high-pressure nappe (northwestern Spain). *Tectonophysics*, 177, 263–292.

Pin, C., Paquette, J.L., Santos Zalduegui, J.F. & Gil Ibarguchi, J.I. 2002. Early Devonian supra-subduction zone ophiolite related to incipient collisional processes in the Western Variscan Belt: The Sierra de Careón unit, Órdenes Complex, Galicia. *In:* Martínez Catalán, J.R., Hatcher, R.D. Jr., Arenas, R. & Díaz García, F. (eds) *Variscan–Appalachian Dynamics: the Building of the Late Paleozoic Basement*. Geological Society of America, Special Papers, 364, 57–71.

Pin, C., Paquette, J.L., Áralos, B., Santos, J.F. & Gil Ibarguchi, J.I. 2006. Composite origin of an early Variscan transported suture: Ophiolitic units of the Morais Nappe Complex (north Portugal). *Tectonics*, 25, 1–19.

Ries, A.C. & Shackleton, R.M. 1971. Catazonal complexes of North-West Spain and North Portugal, remnants of a Hercynian thrust plate. *Nature, Physical Science*, 234, 65–68.

Sánchez Martínez, S. 2009. *Geoquímica y geocronología de las ofiolitas de Galicia*. Nova Terra, 37.

Sánchez Martínez, S., Jeffries, T., Arenas, R., Fernández-Suárez, J. & García-Sánchez, R. 2006. A pre-Rodinian ophiolite involved in the Variscan suture of Galicia (Cabo Ortegal Complex, NW Spain). *Journal of*

the Geological Society, London, **163**, 737–740.

SÁNCHEZ MARTÍNEZ, S., ARENAS, R., DÍAZ GARCÍA, F., MARTÍNEZ CATALÁN, J.R., GÓMEZ BARREIRO, J. & PEARCE, J. 2007*a*. The Careón Ophiolite, NW Spain: supra-subduction zone setting for the youngest Rheic Ocean floor. *Geology*, **35**, 53–56.

SÁNCHEZ MARTÍNEZ, S., ARENAS, R., ANDONAEGUI, P., MARTÍNEZ CATALÁN, J.R. & PEARCE, J.A. 2007*b*. Geochemistry of two associated ophiolites from the Cabo Ortegal Complex (Variscan belt of northwest Spain). *In:* HATCHER, R.D., JR, CARLSON, M.P., MCBRIDE, J.H. & MARTÍNEZ CATALÁN, J.R. (eds) *4-D Framework of Continental Crust*. Geological Society of America, Memoirs, **200**, 445–467.

SÁNCHEZ MARTÍNEZ, S., ARENAS, R., FERNÁNDEZ-SUÁREZ, J. & JEFFRIES, T.E. 2009. From Rodinia to Pangaea: ophiolites from NW Iberia as witness for a long-lived continental margin. *In:* MURPHY, J.B., KEPPIE, J.D. & HYNES, A.J. (eds) *Ancient Orogens and Modern Analogues*. Geological Society, London, Special Publications, **327**, 317–341.

SATO, M., SHUTO, K. & YAGI, M. 2007. Mixing of asthenospheric and lithospheric mantle-derived basalt magmas as shown by along-arc variation in Sr and Nd isotopic compositions of Early Miocene basalts from back-arc margin of the NE Japan arc. *Lithos*, **96**, 453–474.

STAMPFLI, G.M. & BOREL, G.D. 2002. A plate tectonic model for the Paleozoic and Mesozoic constrained by dynamic plate boundaries and restored synthetic oceanic isochrons. *Earth and Planetary Science Letters*, **196**, 17–33.

TONARINI, S., D'ANTONIO, M., DI VITO, M.A., ORSI, G. & CARANDENTE, A. 2009. Geochemical and B–Sr–Nd isotopic evidence for mingling and mixing processes in the magmatic system that fed the Astroni volcano (4.1–3.8 ka) within the Campi Flegrei caldera (southern Italy). *Lithos*, **107**, 135–151.

VERVOORT, J. D. & BLICHERT-TOFT, J. 1999. Evolution of the depleted mantle: Hf isotope evidence from juvenile rocks through time. *Geochimica et Cosmochimica Acta*, **63**, 533–556.

VOGEL, D.E. 1967. Petrology of an eclogite- and pyrigarnite-bearing polymetamorphic rock Complex at Cabo Ortegal, NW Spain. *Leidse Geologische Mededelingen*, **40**, 121–213.

WILLIAMS, I.S. 1997. U–Th–Pb geochronology by ion microprobe: not just ages but histories. *Economic Geology*, **7**, 1–35.

WINCHESTER, J.A., PHARAOH, T.C. & VERNIERS, J. 2002. Palaeozoic amalgamation of Central Europe: an introduction and synthesis of new results from recent geological and geophysical investigations. *In:* WINCHESTER, J.A. PHARAOH, T.C. & VERNIERS, J. (eds) *Palaeozoic Amalgamation of Central Europe*. Geological Society, London, Special Publications, **201**, 1–18.

WOOD, D.A. 1980. The application of a Th–Hf–Ta diagram to problems of tectomagmatic classification and to establishing the nature of crustal contamination of basaltic lavas of the British Tertiary Volcanic Province. *Earth and Planetary Science Letters*, **50**, 11–30.

ZEH, A., GERDES, A., KLEMD, R. & BARTON, J.M. JR, 2007*a*. Archean to Proterozoic crustal evolution in the Central Zone of the Limpopo Belt (South Africa/Botswana): constraints from combined U–Pb and Lu–Hf isotope analyses of zircon. *Journal of Petrology*, **48**, 1605–1639.

ZEH, A., GERDES, A., KLEMD, R. & BARTON, J.M. JR, 2007*b*. U–Pb and Lu–Hf isotope record of detrital zircon grains from the Limpopo Belt—evidence for crustal recycling at the Hadean to early-Archean transition. *Geochimica et Cosmochimica Acta*, **72**, 5304–5329.

ZEH, A., GERDES, A. & BARTON, J.M. JR, 2009. Archean accretion and crustal evolution of the Kalahari Craton—the zircon age and Hf isotope record of granitic rocks from Barberton/Swaziland to the Francistown Arc. *Journal of Petrology*, **50**, 933–966.